Available online at www.sciencedirect.com
SCIENCE DIRECT®
Biochimica et Biophysica Acta 1662 (2004) 42–60
BIOCHIMICA ET BIOPHYSICA ACTA
BBA
www.bba-direct.com

Review

Gap junction channel gating

Feliksas F. Bukauskas*, Vytas K. Verselis

Department of Neuroscience, Albert Einstein College of Medicine, Yeshiva University, 1300 Morris Park Ave., Bronx, New York, NY 10461-1602, USA

Received 24 July 2003; accepted 26 January 2004

Abstract

Over the last two decades, the view of gap junction (GJ) channel gating has changed from one with GJs having a single transjunctional voltage-sensitive (V_j-sensitive) gating mechanism to one with each hemichannel of a formed GJ channel, as well as unapposed hemichannels, containing two, molecularly distinct gating mechanisms. These mechanisms are termed fast gating and slow or 'loop' gating. It appears that the fast gating mechanism is solely sensitive to V_j and induces fast gating transitions between the open state and a particular substate, termed the residual conductance state. The slow gating mechanism is also sensitive to V_j, but there is evidence that this gate may mediate gating by transmembrane voltage (V_m), intracellular Ca^{2+} and pH, chemical uncouplers and GJ channel opening during de novo channel formation. A distinguishing feature of the slow gate is that the gating transitions appear to be slow, consisting of a series of transient substates en route to opening and closing. Published reports suggest that both sensorial and gating elements of the fast gating mechanism are formed by transmembrane and cytoplamic components of connexins among which the N terminus is most essential and which determines gating polarity. We propose that the gating element of the slow gating mechanism is located closer to the central region of the channel pore and serves as a 'common' gate linked to several sensing elements that are responsive to different factors and located in different regions of the channel.

Keywords: Intercellular communication; Connexin; Channel; Voltage and chemical gating

1. Introduction

Connexins (Cxs), a large family of homologous membrane proteins in vertebrates, form gap junction (GJ) channels that provide a direct pathway for electrical and metabolic signaling between cells [1–4]. Each GJ channel is composed of two hemichannels (connexons), which in turn are composed of six Cx subunits. Cxs are predicted to have four alpha helical transmembrane domains (TM1 to TM4), intracellular N- and C-termini, two extracellular loops, and a cytoplasmic loop (CL) [5–7]. Thus far, at least 20 distinct Cx isoforms have been cloned [8]. The existence of multiple Cxs raises the questions of how they differ and how they interact. Unitary conductances of GJs formed of Cx isoforms range from ~ 15 pS (e.g., Cx36) to ~ 300 pS (e.g., Cx37) and channels vary in permselectivity from being nonselective, or being preferentially selective for cations or anions [9].

In invertebrates, GJ channels are formed of innexins, another large family of integral membrane proteins. Despite a lack of primary sequence homology with connexins, innexins form GJ channels with surprisingly similar functional properties [10–13]. Innexin homologues termed Pannexins (Pxs) are also expressed in vertebrates [14]. Three human pannexin genes (Px1, Px2 and Px3) were cloned and it was shown that Px1 and Px2 are expressed in different tissues, while Px3 expression was almost undetectable [15]. In addition, intracellular injection of mRNA encoding the molluscan Px1 substantially increased cell–cell coupling between neurons [16].

Connexin oligomerization into hemichannels occurs in the ER–Golgi and vesicles typically 100–150 nm in diameter transport hemichannels to the plasma membrane [17–24]. Hemichannels themselves can function in the plasma membrane when unapposed or undocked [25,26] and freeze fracture studies performed in *Xenopus* oocytes injected with Cx50 cRNA show hemichannel aggregation into clusters [21] that are similar to those described as 'formation plaques', presumed precursors of junctional plaques, JPs [27]. JP formation has been shown to be regulated by different intracellular regulatory pathways that involve cAMP, G proteins, etc. [28,29].

During the last five years, progress has been made in understanding Cx trafficking, JP formation and internaliza-

* Corresponding author. Tel.: +1-718-430-4130; fax: +1-718-430-8944.
E-mail address: fbukausk@aecom.yu.edu (F.F. Bukauskas).

0005-2736/$ - see front matter © 2004 Elsevier B.V. All rights reserved.
doi:10.1016/j.bbamem.2004.01.008

tion using cells transfected with Cxs fused with green fluorescent protein, GFP [30,31]. By combining fluorescence imaging of Cx-GFPs with dual whole-cell patch recording, it was shown that only channels assembled into JPs are functional, i.e. hemichannels in isolation either do not dock, or if they dock, do not form functional GJ channels [32]. Interestingly, only a fraction (~ 15%) of Cx43-GFP channels in a JP are functional. Our unpublished data show that all other connexins that we have examined (Cx30.2, Cx31, Cx32, Cx36, Cx45, Cx46 and Cx47) show coupling only when JPs are present.

Here, we summarize data related to different forms of GJ channel gating, some of which was elucidated by using GJs assembled of Cxs fused with GFP. GJ channels demonstrate opening and closing transitions in response to voltage, cytoplasmic acidification, changes in intracellular Ca^{2+} concentration, and different chemical compounds known as chemical uncouplers. We describe the evolution of GJ channel gating mechanisms that initiated from voltage gating studies performed ~ 20 years ago in amphibian blastomeres [33,34]. At that time Cxs were not yet cloned and the expanse and sequence diversity of this gene family was unknown. To date, the Cx family contains 20 members, in humans, and cells of different organ-systems frequently co-express several Cxs. Cell–cell communication can be organized through homotypic, heterotypic or/and heteromeric channels that vary highly in conductance, perm-selectivity and gating properties. We postulate that hemichannels, whether unapposed or incorporated into GJ channels, contain two distinct gating mechanisms, called the fast gating and slow or 'loop' gating.

2. Voltage gating

Gap junction channels exhibit a property common among ion channels whereby conductance is sensitive to voltage, i.e., voltage gating. Voltage-sensitive gating can be differentiated into two types, V_j- and V_m-dependent, which represent sensitivities to transjunctional and transmembrane voltages, respectively. These types of voltage dependence can be understood by considering the configuration of the GJ channel, which, by connecting the cytoplasms of adjacent cells, spans both cells' membranes and the intervening extracellular gap between them. The presumed isopotential lines that would result in the GJ channel pore and the channel wall in response to voltages applied to one or both cells are depicted in Fig. 1A–C. When transmembrane voltage, V_m, is equal in both cells (e.g., −50 mV in the example provided, Fig. 1A), then the electric field (E), defined as normal to the isopotential lines, would be oriented across the channel wall and is likely strongest in the region of the intercellular gap. Along the axis of the pore, i.e., in the transjunctional direction, $E=0$. GJ channels that show sensitivity to V_m presumably contain voltage-sensing elements in the channel wall either in the gap or in the transmembrane regions.

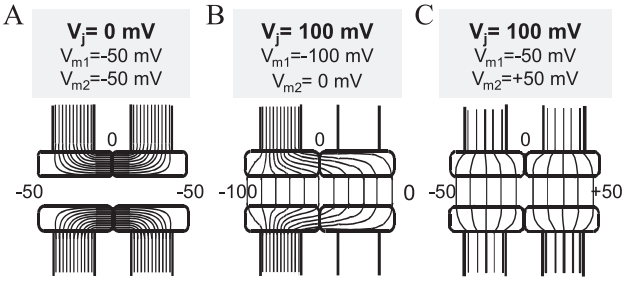

Fig. 1. Schematic representation of a GJ channel with presumed isopotential lines when both cells are held at the $V_j=0$ mV (A), and at $V_j=100$ mV (B & C) but at different values of V_m in each cell. In (A) the channel lumen is isopotential with cytoplasms of both cells; $V_{m1}=V_{m2}=-50$ mV. This condition establishes a strong electric field (E) or a high density of isopotential lines across the channel wall in its central region. No V_j is established and $E=0$ along the channel pore. GJ channels that respond to this voltage profile are termed V_m-sensitive. In (B), V_{m1} differs from V_{m2} establishing a V_j and a constant E along the pore; V_m changes along the channel pore from −100 to 0 mV. In (C), the same V_j and profile of E along the channel pore are established as in (B), but with different values of V_{m1} (−50 mV) and V_{m2} (50 mV). GJ channels that respond the same way to voltage profiles in (B) and (C) are termed V_j-sensitive but not V_m-sensitive.

When the membrane voltages are not equal in both cells, a V_j is established. Shown in Fig. 1B and C are examples of the same V_j (100 mV) generated by: (1) hyperpolarizing one cell to −100 mV (Fig. 1B), or (2) hyperpolarizing one cell to −50 mV and depolarizing the other cell to +50 mV (Fig. 1C). In both cases, E along the channel pore is the same even though the profiles of E across the channel wall are different. GJ channels sensitive only to V_j show the same change in g_j upon hyperpolarizing one cell or depolarizing the other cell to the same degree. Sensitivity to V_j and V_m would lead to different values of g_j for the same V_j, depending on the values of the applied V_ms in both cells.

2.1. V_j-sensitive gating

All GJ channels formed of connexins or innexins show some degree of sensitivity to V_j (for review see Refs. [1,9,35]). Channels formed by connexins generally show the same change in junctional conductance, g_j, by hyperpolarizing one cell or depolarizing the other cell, consistent with sensitivity to V_j and little or no sensitivity to V_m. Although steady-state and kinetic properties of V_j-sensitive gating vary widely among Cxs, a common feature is that steady-state g_j does not decline to zero with increasing V_j, but reaches a plateau or residual conductance that varies from ~ 5% to 40% of the maximum g_j, depending on the Cx isoform [36–43]. An example of g_j–V_j dependence measured in cells expressing Cx43 is illustrated in Fig. 2A. A symmetric reduction in g_j about $V_j=0$ was originally described for GJs between pairs of amphibian blastomeres by Spray et al. [34] and was explained by having identical

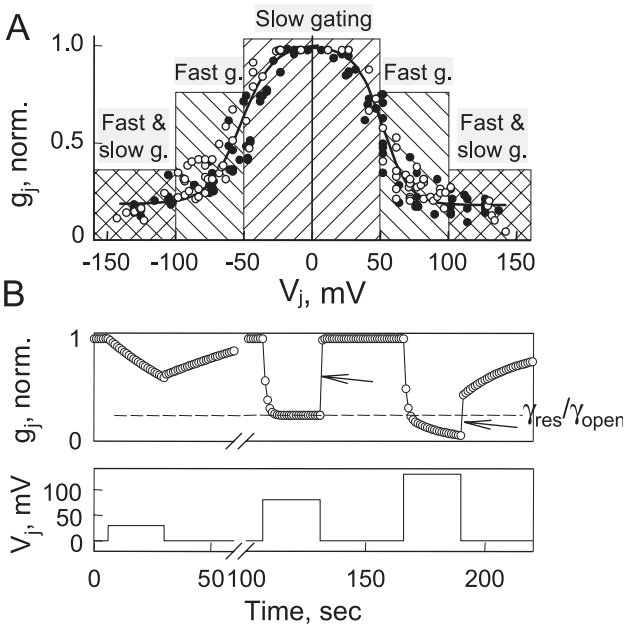

Fig. 2. Voltage gating in HeLaCx43 and Novikoff cell pairs. (A) Pooled data of normalized g_j vs. V_j measured in Novikoff (open circles) and HeLaCx43 (filled circles) cell pairs. The solid line is a fit of all the points to a Boltzmann relation with the following parameters: $V_0 = 51$ mV, $A = 0.08$ mV^{-1} and $G_{min} = 0.2$ for negative V_js and $V_0 = 50$ mV, $A = 0.09$ mV^{-1} and $G_{min} = 0.18$ for positive V_js. Squares filled with lines of different orientations indicate areas in which V_j gating is mediated predominantly through the slow gate (rising lines), the fast gate (declining lines) and both gates (crossing lines). (B) Schematic drawings of g_j evaluated over time in response to V_j steps varying in amplitude from ~ 30 to 150 mV that exemplify our findings in cells expressing Cx43 (see Fig. 1 in Ref. [51]). When V_j steps are < 50 mV (see g_j and V_j traces in 0–60-s interval), g_j declines and recovers slowly. When V_js are in the range of ~ 50–100 mV (see g_j and V_j traces in 50–150-s time interval), g_j declines fast reaching steady state in few seconds. Recovery of g_j is also fast. At $V_j > 100$ mV, the decline in g_j is very fast initially and continues to decline more slowly without reaching steady state in the time interval shown (see g_j and V_j traces in 150–220-s interval).

V_j-sensitive gates in each hemichannel such that for each polarity of V_j, closure can be ascribed to one or the other hemichannel [33]. The macroscopic residual conductance, also referred to as G_{min}, was explained by suggesting that there was either a parallel voltage-insensitive conductance or that rate constants governing opening and closing reached a plateau with V_j leaving a non-zero open channel probability (p_o).

2.1.1. Evidence for two V_j-sensitive gating mechanisms in GJ channels

Single GJ channel recordings in insect cells not only provided an explanation for the macroscopically observed G_{min} characteristic of V_j-dependence, but also raised the possibility that GJs possess more than one voltage gating mechanism [44–46]. When two insect cells, obtained from a cell line derived from the mosquito, *Aedes albopictus*, were patch-clamped and placed into contact to observe the formation of electrical coupling, the appearance of the first channel was characterized by an apparent slow rise in junctional current (I_j) from a non-conducting state to an open state or the main state. Occasionally, the slow rise in I_j could be seen to consist of multiple step changes en route to full opening, sometimes taking tens of milliseconds for a channel to open fully. Once opened, the channel responded to V_j with gating transitions between the open state, γ_{open}, and a long-duration substate, i.e., the channel did not close completely. In contrast to the slow or stepwise initial opening, the transitions to and from the substate were fast and more typical to ion channel gating. For these insect GJs, the substate amplitude was ~ 20–25% of the fully open state and suggested that the macroscopic residual conductance or G_{min} could be explained by incomplete closure of GJ channels [44–46]. On occasion, gating transitions to the fully closed state and back were observed and were characterized by slow transition times (~ 10 ms). Such slow gating transitions were similar to the opening transitions observed during de novo channel formation and were observed more frequently during depolarization of both cells, or exposing cells to chemical uncouplers (see Sections 2.2 and 3).

Cloning of connexins and their expression in exogenous systems allowed examination of individual GJ channels and showed that, indeed, GJ channels formed of connexins similarly failed to close completely with V_j, i.e., the channels gated to a subconductance state [36,47–51]. The incompletely closed state is now generally referred to as the residual conductance state, γ_{res}, and the macroscopic parameter G_{min} can be attributed to the summed conductances of all the GJ channels residing in γ_{res}. In addition, GJ channels formed from connexins as well as innexins occasionally gated to a completely closed (non-conducting) state, referred to as γ_{closed}. The full closures consisted of slow or multi-stepped transitions similar to those observed during de novo channel formation and V_m-sensitive gating. Interestingly, similar full closure of the channel with slow or multi-stepped transitions could be induced by application of a number of chemical agents, including long-chain alkanols, anesthetics, arachidonic acid, CO_2, etc [50,52,53], suggesting that stimuli which induce slow gating transitions to and from γ_{closed} may operate through a common gate (see Section 4), acted upon by various effectors. The two putative gates, V_j-sensitive and the common gate, were called fast and slow gates, referring to the fast and slow gating transitions that characterize them [46,50]. Initially it was thought that V_j-sensitive gating occurs exclusively by the fast gate. However, it was subsequently shown that V_j can also initiate slow gating transitions to γ_{closed} [51,54]. This finding led to the conclusion that fast and slow gates are both sensitive to V_j.

Studies of unapposed Cx hemichannels similarly suggest that there are two distinct voltage gating mechanisms [26]. Cx46 hemichannels exhibit slow gating transitions between open and fully closed states at inside negative voltages,

while at inside positive voltages gating transitions are fast and between the open state and a substate. Based on the similarity of the slow gating transitions at inside negative voltages to those observed during de novo channel formation [46], it was suggested that the extracellular loops may be involved and the slow gating mechanism was provisionally called 'loop' gating. For inside positive voltages, gating to the substate was ascribed to the fast gate. In the case of unapposed Cx46 hemichannels, the two gating mechanisms have different gating polarities, the slow or 'loop' gate closing at inside negative voltages and the fast gate at inside positive voltages.

2.1.2. Properties of V_j-sensitive gating

V_j dependence examined in Cx43 GJ channels shows that g_j declines substantially at V_js between ± 30 and ± 80 mV to a level close to the residual conductance, but then continues to decline, albeit less steeply, towards zero at larger V_js (Fig. 2A). In examining the kinetics of the changes in g_j at various V_js, slow kinetics (reduction and recovery) is observed at small V_js, <50 mV (left g_j trace in Fig. 2B; note that during the $\sim$25-s V_j step applied, g_j did not reach steady state). At V_js between $\sim$50 and $\sim$100 mV (middle g_j trace in Fig. 2B), kinetics of decay and recovery is rapid and g_j reaches a steady-state value that approximates the ratio, $\gamma_{res}/\gamma_{open} = 25$ pS/110 pS = 0.23 consistent with channels closing to the residual conductance state. At large V_js, typically >100 mV (right g_j trace in Fig. 2B), a fast decline in g_j occurs and is followed by a slow decline; note that g_j does not reach steady-state during the duration of the V_j step. Recovery also consists of two phases, a rapid increase in g_j followed by a considerably slower increase towards pre-step values. Correlative single channel studies (Fig. 3) show that slow V_j gating is largely responsible for the changes in g_j at small V_js (<50 mV). In the example shown ($V_j = 37$ mV), most gating transitions were 110 pS in amplitude, representing transitions between γ_{open} and γ_{closed}; transitions to γ_{res} ($\sim$85 pS) were observed, but were infrequent (Fig. 3B; see Ref [51] for more details). At intermediate V_js between $\sim$60 and $\sim$80 mV, I_j declines rapidly, predominantly through $\sim$85-pS transitions, representing gating from γ_{open} to γ_{res} (Fig. 2C and D). In contrast to that which occurs at small V_js, closures to γ_{closed} are infrequent. For the 75-mV V_j step shown (Fig. 3D), I_j declined exclusively through $\sim$85-pS transitions to reach a current corresponding to that expected if all Cx43 channels resided in γ_{res}. At large V_js (107 mV in Fig. 3E), I_j exhibited a very fast decline (not resolved with the time scale shown) to a level corresponding to that expected if all channels resided in γ_{res}, indicating gating from γ_{open} to γ_{res}. However, unlike at 75 mV where I_j remained at the residual conductance level, I_j continued to decline, via $\sim$25-pS gating transitions (see inset). Thus, at large V_js, the fast recovery reflects the fraction of channels closed by the fast gate and the slow component those closed by the slow gate. The kinetics of g_j recovery can be informative in determining the fractions of channel closed by fast and slow gating mechanisms.

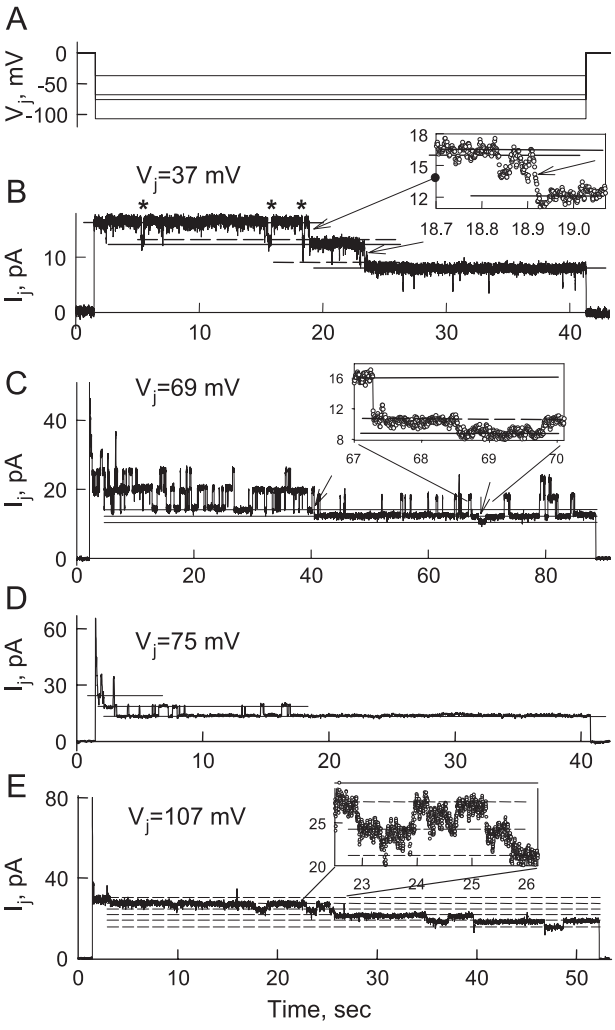

Fig. 3. $g_j - V_j$ dependence of Cx43 at the single channel level. (A) V_j steps applied to individual cell pairs. (B–E) I_j responses to V_j steps of 37 mV (B), 69 mV (C), 75 mV (D) and 105 mV (E). With a V_j step of 37 mV (B), four channels open at the beginning of the step and two closing transitions occur between open and closed states of $\sim$110 pS (arrows) during the duration of the step. Also evident are several brief transitions, $\sim$85 pS in magnitude (asterisks) representing transitions to the residual conductance state (γ_{res}). An expanded time scale (inset; sampling interval 1 ms) shows that the $\sim$110-pS transitions are slow, taking several milliseconds to fully close the channel. At $V_j = 69$ mV (C), I_j declines rapidly through stepwise transitions of 85 pS indicating that the decline in g_j is via gating to γ_{res}. One channel undergoes a full 110-pS closing transition (first arrow). Also evident is a small 30-pS slow transition ascribable to a full closure of a channel from γ_{res} (second arrow; also see inset, sampling interval, 5 ms). At $V_j = 75$ mV (D), all the channels rapidly close to the residual state with transitions of 85 pS. At $V_j = 107$ mV (E), I_j declines very rapidly to a level that corresponds to all channels residing in γ_{res} and is followed by a slow decline in I_j through stepwise 30-pS transitions corresponding to full channel closures from γ_{res}. The expanded time scale (inset; sampling interval, 2 ms) shows the 30-pS transitions to be slow, taking several milliseconds to complete. Adapted from Ref. [51].

These studies have led to a revised picture of V_j gating in GJ channels as follows. Each hemichannel in a GJ

channel has two gate/sensor complexes arranged serially in the pore. Because V_j acts on both gates, closure of one gate largely collapses V_j across it, thereby changing V_j across the other gate. Thus, the open probability of one gate is dependent on the state of the other through changes in the local field, interdependence between the gates termed contingent gating by [33]. In Cx43, the slow V_j gate is less steeply sensitive to V_j than the fast V_j gate, but shifted such that it closes at smaller V_js. Thus, small V_js induce modest changes in g_j mediated by closure of the slow gate. Larger V_j steps tend to first close the fast V_j gates because they have faster gating (closing) kinetics. Consequently, a major fraction of V_j drops across the fast V_j gate, leaving only a small fraction across the voltage sensor of the slow V_j gate. This essentially 'eliminates' the slow gate from operation, giving the appearance that slow V_j gating is absent at intermediate V_js. At larger V_js, the small V_j fraction is sufficient to close the slow V_j gate even with the fast V_j gate closed giving rise to a continued decline in g_j towards zero. Squares filled with lines of different orientation shown in Fig. 2A summarize our view of the different degrees to which fast and slow gating mechanisms are involved in V_j-sensitive gating depending on V_j amplitude. In different connexins, differences in V_j sensitivity and relative shifts along the V_j axis of fast vs. slow V_j-sensitive gating can produce a variety of g_j–V_j relations as a result of contingent interactions.

Because a major difference between the two gating mechanisms is the appearance of the respective gating transitions [50], it was important to characterize them quantitatively. Fig. 4A shows that a frequency histogram of fast V_j gating transitions measured between open and residual states is in the range of ~1–4 ms. Presumably many of those measuring 1 ms are actually shorter, but their measurement was limited by the recording system. For slow V_j gating between fully open and closed states, transitions are in the range of ~2–25 ms (Fig. 4B). Although there is some overlap, the mean values of the transitions ascribed to the two gating mechanisms differ substantially, 2.0 ± 0.2 vs. 11.5 ± 0.6 ms. These relatively slow gating transitions appear to consist of a series of transient sub-transitions that may represent conformational changes in individual subunits that are stable enough to have measurable lifetimes. Open and closed states may represent all six subunits in open or closed conformations, respectively. Conversely, fast V_j gating may involve conformational changes in subunits that are too fast to resolve individually or conformational changes initiated in a single connexin molecule that lead to rapid closure [55]. A "cork" model has also been proposed for fast V_j gating in which one calmodulin molecule interacting with single connexin molecule transfers a channel to the residual state [56].

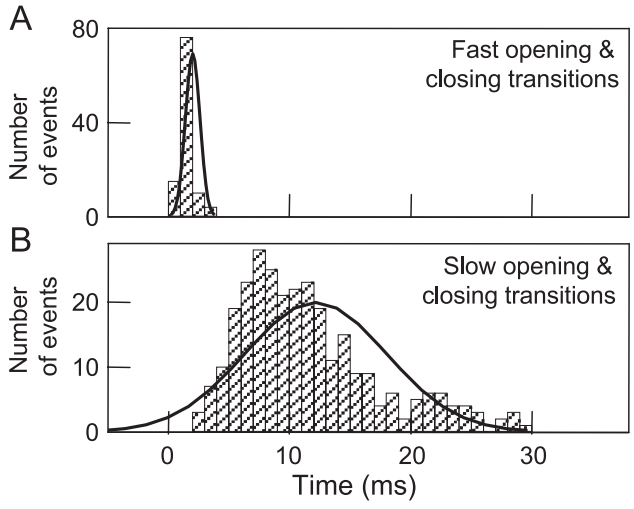

Fig. 4. Frequency histograms of I_j transition time between open and residual states (A) and between open and closed states (B). Data were collected from fibroblasts and HeLa-43 cells at V_js ranging from 25 to 75 mV during transient uncoupling by bath application of CO_2. Solid lines are Gaussian curves that fit to the data with mean values of 11 ± 0.8 ms ($n = 264$) and 2.0 ± 0.2 ms ($n = 105$) for upper and bottom plots, respectively. Adapted from Ref. [50].

We should point out that the residual conductance state is only one substate among a number that have been observed both in insect and mammalian GJ channels. However, the residual conductance state is distinguished by its frequent occurrence and its long dwell times, both of which increase with V_j.

Studies using EGFP attached to the carboxy terminus of Cx43 provided additional evidence for two gating mechanisms and a molecular distinction between them. In Cx43-EGFP channels, there is a selective disruption of fast V_j gating leaving slow V_j-gating intact [32]. Whereas a single Cx43 channel exhibits gating between open and residual states (Fig. 5A), a single Cx43-EGFP channel gates only between open and closed states (Fig. 5B). In heterotypic Cx43/Cx43-EGFP channels, V_j gating is asymmetric with only slow V_j gating observed for V_js relatively negative on the Cx43-EGFP side and both fast (see dashed lines) and slow (they were rare and not present in this example) V_j gating for V_js relatively negative on the wtCx43 side (Fig. 5C). Thus, both forms of V_j gating segregate with the corresponding hemichannels consistent with their being hemichannel properties. The V_j polarity that closes both fast and slow V_j gates in Cx43 hemichannels is that which is relatively negative on the cytoplasmic side.

2.1.3. Permselectivity of the residual state

Oh et al. [57] demonstrated that although the open channel current of Cx32 is linear with V_j, the residual state rectifies such that current increases when the closed hemichannel is made relatively more negative. They concluded that this observation is consistent with an increase in the electrostatic effect of a positive charge positioned at the cytoplasmic vestibule of the gated hemichannel. We examined whether the residual state of the Cx43 channel also exhibits rectification. Furthermore, we extended these studies to examine whether the Cx43 channel in the residual

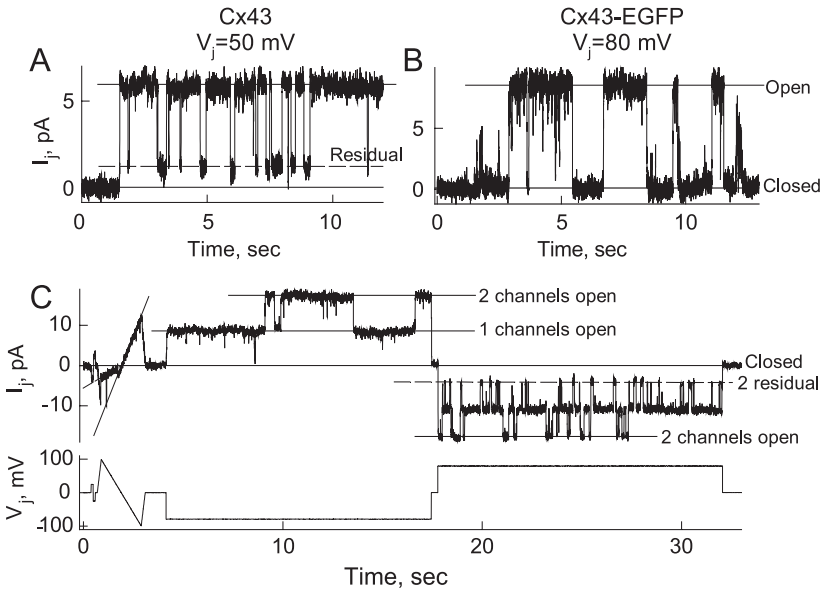

Fig. 5. Voltage gating of wild-type Cx43 differs from that of Cx43-EGFP. (A–B) Single GJ channel gating transitions at $V_j = 50$ mV for Cx43 (left) and at $V_j = 80$ mV for Cx43-EGFP (right) expressed in HeLa cells. For Cx43, gating transitions are between open (solid line) and residual (dashed line) conductance states; full closures (not shown) occurred but were infrequent. For Cx43-EGFP, gating transitions are only between open and fully closed states. (C) Asymmetric V_j gating in heterotypic Cx43/Cx43-EGFP junctions. Shown are currents recorded from a cell pair containing two functional channels in response to a ± 100-mV ramp and ± 80-mV V_j steps applied to the HeLaCx43-EGFP cell. For the − 80-mV V_j step, only gating transitions of ~ 110 pS between open and closed states are observed, whereas for the + 80-mV V_j step, gating transitions of ~ 85 pS occur between open and residual states (dashed lines). Adapted from Ref. [51].

state represents a narrowed pore and whether there is a change in the charge selectivity compared to the open state.

It is well established that open Cx43 channels are poorly charge selective, exhibiting permeability to both mono- and divalent negatively and positively charged dyes [2,58–61]. We found that Cx43-EGFP channels are also permeable to all these dyes, indicating that attachment of EGFP to the C-terminus does not alter Cx43 selectivity. In addition, we demonstrated that Cx43-EGFP channels are permeable to APTS (8-aminopyrene-1,3,6-trisulfonic acid, trisodium salt; MW 523 Da), which has three negative charges (Fig. 6). However, not all GJ channels show poor charge selectivity like Cx43. Cx32 channels are preferentially permeable to negatively charged dyes, whereas Cx46 channels are preferentially permeable to positively charged dyes [61].

To explore the permeability of the residual state of Cx43 GJs to dyes, we used the V_j 'window' between 60 and 90 mV at which most channels close to the residual state via the fast gate (see Figs. 2 and 3). Also, we modified the traditional dual whole cell voltage clamp protocol in cell pairs by adding a third pipette to load one cell with dye when GJ channels were in the residual state. Fig. 7A shows a phase-contrast image of a cell pair with three pipettes outlined by dashed lines. After gigohm seals were formed with all three pipettes, whole-cell recordings were established with pipettes 1 and 2. Both pipettes were held at a common voltage to maintain $V_j = 0$ mV. A g_j of 43 nS, corresponding to ~ 390 open channels, was measured by applying repeated small, brief V_j steps. A long-duration 90-mV V_j step was then applied to cell 2 (Fig. 7D). Given the polarity of closure of the fast V_j gate in Cx43 hemichannels, this V_j step would tend to close the Cx43 hemichannels in cell 1. Upon reaching the steady-state residual current, the patch in the third patch pipette (attached to cell 1) filled with Alexa Fluor was ruptured to initiate dye loading (solid arrow). Fluorescent image taken 15 s after the start of dye loading is shown in Fig. 7B. The time courses of the fluorescence changes in both cells are plotted in Fig. 7C. Fluorescence intensity rapidly rose in cell 1 after opening the dye-filled patch pipette, but almost no fluorescence was detected in cell 2. V_j was such that cell 2 was relatively positive which would assist transfer of the negatively charged Alexa Fluor. Upon removal of V_j (dashed arrow), conductance rapidly recovered as channels fully opened and fluorescence immediately started to rise in cell 2 concomitant with a decrease in cell 1. These results are indicative of rapid flux of dye from cell 1 into cell 2 in the absence of V_j. A second depolarization of cell 2 by 90 mV again halted dye flux into cell 2; the decrease in fluorescence in cell 2 is likely due to dye loss into the patch pipette.

These data show that the high permeability of open Cx43 channels to Alexa Fluor is virtually abolished (or reduced below detection) in the residual state. Intercellular flux of Alexa Fluor was affected much more than predicted by the change in conductance. We obtained similar results by examining cell–cell transfer of the positively charged dye, ethidium bromide. No transfer of ethidium bromide was detected in well-coupled cell pairs with channels in the residual state, whereas dye transfer was evident in the absence of V_j (for details see Fig. 8 in Ref. [62]).

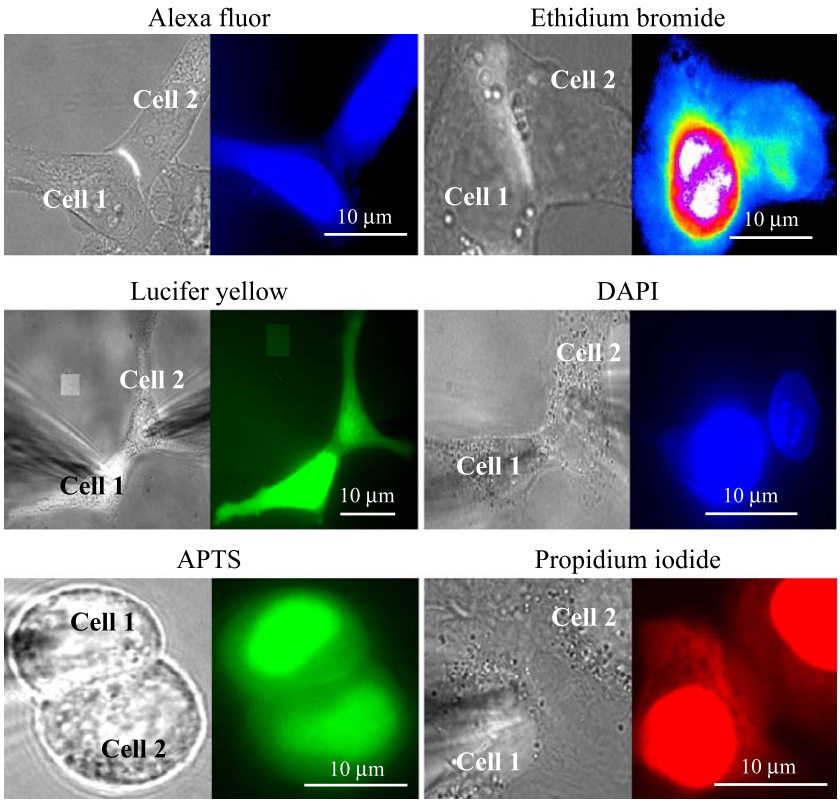

Fig. 6. Cx43-EGFP channels are permeable to negatively (*Alexa fluor*$^{(1-)}$, *Lucifer yellow*$^{(2-)}$, *APTS*$^{(3-)}$) and positively (*Ethidium bromide*$^{(+)}$, *DAPI*$^{(2+)}$ and *propidium iodide*$^{(2+)}$) charged dyes. In all examples shown, the HelaCx43-EGFP cell pairs demonstrated at least one junctional plaque in the region of cell–cell contact. In all cases, the cell designated as cell 1 was patched with pipette containing dye. Images were recorded ~ 10 min after establishing a whole cell recording in cell 1. After allowing ~ 10 min for dye transfer, electrical cell–cell coupling was evaluated by establishing a whole-cell recording in cell 2 with the second pipette. All the cell pairs shown responded to heptanol (2 mM) treatment with uncoupling, which indicates that GJs and not cytoplasmic bridges were responsible for the dye transfer.

We also demonstrated that the $I–V$ relation of an open Cx43 channel is linear while that of the residual state shows rectification with γ_{res} decreasing as V_j is made increasingly positive on the side of gated hemichannel. Based on modeling studies performed with Poisson–Nernst–Plank (PNP) theory [63], we suggested that the rectification of the residual state can be explained by introduction of positive charge in the pore. Fitting experimental data to the model suggested that the positive charge is most likely located close to the cytoplasmic vestibule of the gated hemichannel as proposed for Cx32 in Ref. [57]. To assess selectivity, we substituted either K^+ with TEA^+ or Cl^- with $Aspartate^-$ in patch pipettes. These substitutions resulted in a substantial reduction γ_{open} and can be explained if both K^+ and Cl^- contribute substantially to the current flowing through the open channel, consistent with our previous studies using measurements of E_{rev} in KCl gradients that showed no appreciable selectivity between monovalent inorganic ions on the basis of charge [64]. The same substitutions had substantially different effects on γ_{res} and we found that closure to the residual state converts Cx43 from being nonselective to being preferentially selective for anions [62].

Although the introduction of charge can explain the appearance of rectification and change in charge selectivity, it cannot obviously explain the small conductance of the gated channel, which is ~ 5 times smaller than that of the open state, or the apparent impermeability to fluorescent dyes. Thus, the conformational change associated with fast V_j gating to the residual state must also lead to a significant narrowing of the channel pore, which substantially decreases conductance and reduces the cutoff size for permeant molecules. Our data indicate that molecules similar in size to fluorescent dyes (~ 400 Da) would be excluded. A similar conclusion was made based on dye and cAMP transfer studies performed in *Xenopus* oocytes expressing Cx43 or Cx46 [65]. Consequently, the fast V_j gating mechanism can serve as a 'selectivity filter that preserves electrical cell–cell communication but limits the communication of metabolic or biological signaling molecules'.

2.1.4. What is known about molecular mechanisms of fast V_j gating?

Mutational studies of Cx26 and Cx32 demonstrated that the gating polarity of the fast gating mechanism is governed by charged residues in the N-terminal domain

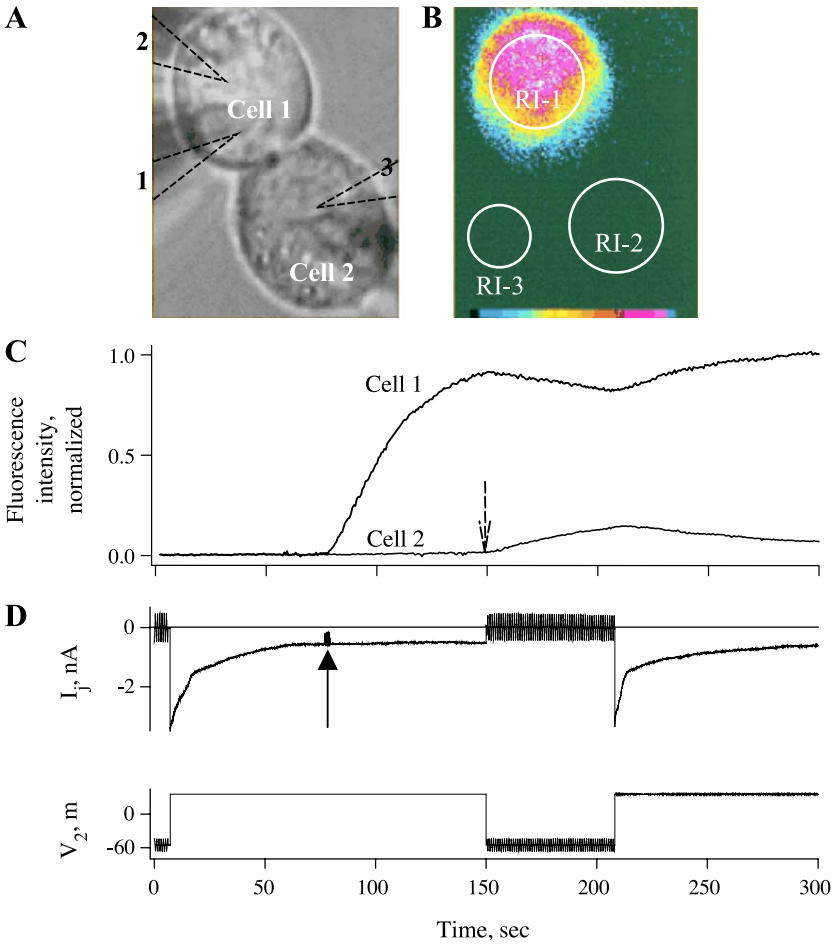

Fig. 7. Intercellular transfer of Alexa Fluor, a negatively charged dye, is restricted when channels are in the residual state. (A and B) Phase-contrast (A) and fluorescence (B) images showing a Novikoff cell pair in which dye transfer and electrical coupling were examined in open and residual states. Locations of pipettes 1 and 2 used for dual whole-cell recording and pipette 3 used for loading cell 1 with dye are indicated. RI-1, RI-2, and RI-3 are regions of interest from which fluorescence intensities were measured over time. Fluorescence intensities in the cells (RI-1 and RI-2) were calculated by subtracting the background fluorescence (RI-3). (C) Plot of normalized fluorescence intensity (FI) in cell 1 and cell 2 over time. A V_j of +90 mV was imposed causing a decline in I_j to the residual conductance. Opening the patch in pipette 3 at steady state of g_j (see solid arrow) causes FI in cell 1 to rise. FI in cell 2 shows no change during the time when channels mainly reside in the residual state. Upon reopening channels by removal of V_j (see dashed arrow), FI begins to rise immediately in cell 2 and reaches ~ 14% of the maximum within 60 s. Imposition of V_j a second time caused an immediate decline in FI in cell 2 due to loss of transfer from cell 1 and dialysis with patch pipette 2. (D) Records of I_j and V_2 over time corresponding to fluorescence plot in (C). The V_j of +90 mV imposed by stepping the voltage in cell 2 caused g_j to decline from 43 nS to a steady-state value of ~ 10 nS. Between the +90-mV V_j steps, small repeated ± 10-mV V_j steps were applied to cell 2 to measure g_j. I_j recovered rapidly upon removal of the V_j step, indicating that mainly the fast gate was operating. Adapted from Ref. [62].

[66,67] and that this polarity could be reversed independent of the slow gating mechanism [55]. In cell–cell channels, modifications of Cx43, including deletion of the CT domain [43] or attachment of aequorin or EGFP to CT [32,68], selectively abolishes fast V_j gating, leaving the slow gating mechanism intact. In addition, it was proposed that the fast V_j gate initiates a kink of the second transmembrane domain that narrows the pore at the cytoplasmic end [66]. Studies show that positive charges positioned near the cytoplasmic ends of Cx32 and Cx43 channels can explain current rectification in the residual state and selectivity properties [55,62]. These data are consistent with a mechanism proposed for fast V_j gating which suggest that the V_j sensor is composed of a charge complex located in the N-terminus whose net charge can be of either sign, and whose movement towards the channel pore is associated with hemichannel closure to the residual state [55]. To date, the data support the view that the sensor/gate complex of the fast V_j gate is located at the cytoplasmic end of each hemichannel.

2.1.5. V_j gating of heterotypic GJ channels

Heterotypic channels are composed of docked hemichannels that differ in connexin composition. The component hemichannels can have substantially different open and residual state conductances. Although single open channel I – V relations of homotypic channels are usually linear, asymmetry in structure of heterotypic channels frequently is accompanied by a rectifying I–V relation [48,67,69].

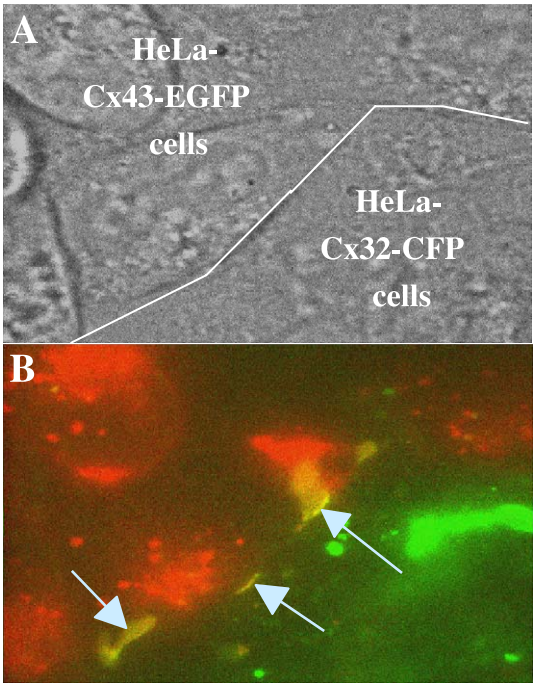

Fig. 8. Cx32-CFP and Cx43-EGFP form heterotypic junctions visible as large junctional plaques. (A) A phase-contrast image of HeLa cells expressing Cx43-EGFP (on top of white line) and Cx32-CFP (below white line). (B) A color overlay of fluorescence images of HeLaCx32-CFP shown in green and HeLaCx43-EGFP cells shown in red. The arrows indicate heterotypic junctional plaques (yellow regions).

Only some combinations of connexins appear to be capable of forming functional heterotypic channels. Compatibility among different connexins was intensively studied in oocytes [37,40,70] as well as in mammalian [48,71–73] and insect cell lines [74]. There are 190 possible types of heterotypic channels that can be formed from the 20 Cx isoforms and only a fraction of them has been examined for compatibility. Several Cx isoforms do not appear to function as homotypic channels, e.g., Cx31.1 and Cx29, but it is not clear whether they function as heterotypic channels when paired with other Cxs. For example, Cx29 when co-expressed with Cx32 has been reported to form functional heteromeric channels [75].

Functionally incompatible connexins may actually be structurally compatible in their ability to dock and cluster into junctional plaques, but unable to open. For example, it was reported that Cx32 and Cx43 do not form functional heterotypic channels when expressed in oocytes [40]. However, when examining co-cultures of HeLaCx32-CFP and HeLaCx43-EGFP expressing cells, we found large Cx32-CFP/Cx43-EGFP junctional plaques (Fig. 8); functional coupling of these cell pairs has not yet been examined. Asymmetry in gating in heterotypic junctions allows examination of gating polarity, a property obscured by the symmetric nature of gating in homotypic channels. The polarity of slow V_j gating appears to be negative in all connexins examined thus far, which includes Cx32, Cx43, Cx45, Cx46 and Cx50 [55,61,76], and may be a conserved property among connexins. We believe that the slow V_j gating mechanism is largely responsible for maintaining undocked or unapposed hemichannels closed at physiological resting potentials. The gating polarity of the fast V_j gate is Cx type-dependent. For example, the gating polarity of the fast gate of Cx37, Cx40, Cx46 and Cx50 is positive, while in Cx32, Cx43 and Cx45 is negative (for review see Refs. [9,35]).

To study gating mechanisms of heterotypic channels, we used the Cx45/Cx43-EGFP channel because an absence of the fast V_j gate in the Cx43-EGFP hemichannel significantly simplifies data interpretation. Homotypic Cx45 junctions show a steep decline in g_j about $V_j = 0$ that reaches a minimum at ± 50 mV and then a slight increase at increasingly larger V_js (see inset in Fig. 9A). Our studies show that in Cx45/Cx43-EGFP heterotypic junctions, steady-state $g_j - V_j$ dependence is highly asymmetric (see Fig. 9B). There is a steep decline in g_j at V_js positive to the Cx43-EGFP side up to ~ 50 mV, and then a slight increase at larger V_js (see inset), as seen for either polarity of V_j in homotypic Cx45 junctions. For V_js negative on the Cx43-EGFP side, g_j increases to reach a peak at ~ -30 mV, and then decreases. Single channel studies show that the Cx45 hemichannel is largely responsible for the changes in g_j between the maximum at $V_j = -30$ mV and the minimum at $V_j = +50$ mV, and gating is predominantly via the slow V_j gating mechanism (Fig. 9C and D). Over this V_j range, the fast V_j gate in the Cx45 hemichannel stays open. At larger V_js positive to the Cx43-EGFP side, fast V_j gating to the residual state in the Cx45 hemichannel can be seen to occur (Fig. 9D). Closure of the fast V_j gate at these larger V_js reduces V_j at the slow gate, which tends to keep it open and gives rise to the secondary increase in g_j (see insert in Fig. 9B). At small negative V_js on the Cx43-EGFP side, channels open with slow opening transitions (an example is shown in Fig. 9C), which underlies the increase in g_j towards the peak observed macroscopically. These data indicate that at $V_j = 0$ mV, a substantial fraction ($\sim 1/3$ in this case) of Cx45/Cx43-EGFP channels are closed by the slow V_j gate in the Cx45 hemichannel; both the fast V_j gate in the Cx45 hemichannel and the slow V_j gate in the Cx43-EGFP hemichannel are open. The slow gate of Cx43-EGFP hemichannel begins to close only at larger V_js, negative to the Cx43-EGFP side, resulting into a decrease in macroscopic g_j. The low V_j gating sensitivity of Cx43-EGFP hemichannel is explained by the small fraction of V_j that it sees; the Cx43-EGFP hemichannel has a ~ 3.5-fold higher conductance compared to the Cx45 hemichannel. This factor would virtually reduce V_j sensitivity of Cx43 hemichannel and increase V_j sensitivity of Cx45 hemichannel, and explains a higher V_j sensitivity of Cx45 when incorporated into a Cx43/Cx43-EGFP channel (see right shoulder of $g_j - V_j$ plot in Fig. 9B) when compared with

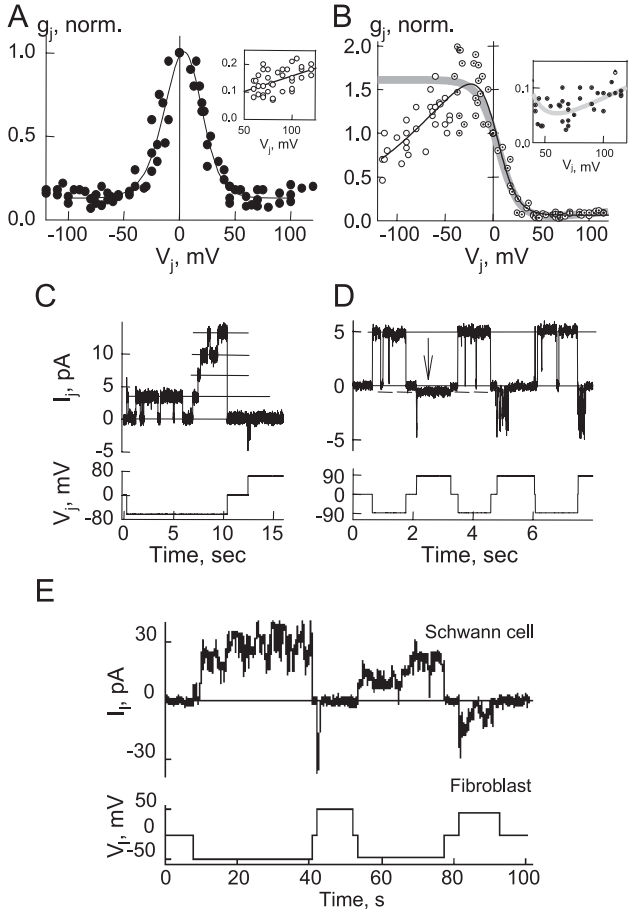

Fig. 9. Asymmetric V_j gating in heterotypic Cx45/Cx43-EGFP junctions. (A) Pooled data of normalized steady-state g_j (G_j) vs. V_j measured in 15 homotypic HeLaCx45 cell pairs. The solid line is a fit of all of the data points to a contingent gating model containing one gate per hemichannel with parameters $A=0.3$ mV^{-1} and $V_o=8.9$ mV for negative V_j, and $A=0.17$ mV^{-1} and $V_o=7.5$ mV [76]. The value of g_j reaches a minimum at ± 60 mV and then increases at higher V_js (inset; the solid line is a regression line of the first order). (B) Normalized g_j-V_j relation of a Cx45/Cx43-EGFP heterotypic junction. Data were pooled from 14 cell pairs. The thin black line is a fit of all data points to a four-state contingent gating model with one gate in each hemichannel (open and dotted circles). The parameters are $A=0.18$ mV^{-1} and $V_o=1$ mV for the Cx45 hemichannel and $A=0.03$ mV^{-1} and $V_o=26$ mV for the Cx43-EGFP hemichannel. The thick gray line is a fit of the data points indicated by dotted circles to a four-state contingent gating model of the channel containing fast and slow gates only in the Cx45 hemichannel. The parameters are $A=0.27$ mV^{-1} and $V_o=3$ mV for the slow gate and $A=0.46$ mV^{-1} and $V_o=10$ mV for the fast gate. An expanded view (inset) demonstrates that the contingent model can explain the secondary increase in g_j at large V_js [76]. (C) Example of opening of Cx45/Cx43-EGFP channels during a V_j step of -60 mV applied to the Cx43-EGFP cell. Gating transitions are slow and between open and closed states. During a subsequent V_j step of $+60$ mV, channels close completely with a short latency. (D) During V_j steps of 90 mV negative on Cx43-EGFP side, Cx45/Cx43-EGFP channels gate between the open state with a conductance of ~ 55 pS and the fully closed state. During positive V_j steps, the channel gates to the residual state (see arrow and dashed line) or to the closed state (second and third positive steps). (E) An example of asymmetric V_j gating in a Schwann/Fibroblast cell pair in response to V_j steps of ± 50 mV. Adapted from Ref. [76].

g_j-V_j dependence of a homotypic Cx45 channel (see Fig. 9A). The asymmetry described here resembles that found in junctions formed between fibroblasts and Schwann cells isolated from sciatic nerve of 1-day-old neonatal rats (Fig. 9E), suggesting that Cx45/Cx43 junctions may form in vivo [77].

Modeling studies, based on the contingent gating model of the channel containing fast and slow V_j gates in series, showed that the slow gate in the Cx45 hemichannel would be largely responsible for closure of Cx45/Cx45 or Cx45/Cx43-EGFP channels at $V_j=0$ [76]. Assuming that both hemichannels operate independently, $\sim 50\%$ of Cx45/Cx45 channels and $\sim 30\%$ of Cx45/Cx43-EGFP channels should be closed at $V_j=0$ mV. Modeling studies also show that pairing hemichannels differing in unitary conductance should reduce the V_j sensitivity of the hemichannel with higher conductance and vice versa, and this can shift g_j-V_j dependence so substantially to give the appearance that pairing induces novel gating properties [43,78].

2.1.6. Signal transfer asymmetry in heterotypic junctions

We examined electrical cell–cell coupling in HeLaCx45/HeLaCx43-EGFP cell pairs by voltage clamping one cell and current clamping the other. Fig. 10A and B illustrates an experiment in which the voltage in the HeLaCx43-EGFP cell was clamped to a holding potential (V_{h1}) of 0 mV and to which repeated (3 Hz) positive or negative voltage steps (30 ms in duration and 100 mV in amplitude) were applied. Prior to the record, the holding current in the HeLaCx45 cell was set to keep the holding potential, V_{h2}, at $\sim +5$ mV. During application of -100-mV pulses to the Cx43-EGFP cell, the response in the Cx45 cell reached ~ -60 mV, giving a coupling coefficient for the pulses, $k_{1-2,-}=V_2/V_1$ of ~ 0.6. When positive pulses were applied the Cx43-EGFP cell, the initial response in the Cx45 cell was about 20 mV, but diminished over several seconds to reach a steady-state value of ~ 10 mV resulting in $k_{1-2,+}=\sim 0.1$. The ratio of coupling coefficients for positive and negative V_j, $k_{1-2,+}/k_{1-2,-}$, which we defined as the electrical coupling asymmetry coefficient, $K_{asym}=\sim 0.17$. When the holding current in the Cx45 cell was made more negative ($\sim$ 19th s on time scale in Fig. 10A), the initial response in the Cx45 cell for -100-mV steps applied to the Cx43-EGFP cell increased from an initial value ~ 20 mV to reach of ~ 60 mV superimposed on the steady voltage. When positive pulses were applied to the Cx43-EGFP cell, the responses in the Cx45 cell rapidly decreased to about ~ 3 mV, so that $K_{asym}=0.05$. These data demonstrate that a small difference between holding potentials of two cells, $\Delta V_{jh}=V_{h1}-V_{h2}$, can strongly influence the asymmetry of electrical coupling. Fig. 10C shows a summary of the data illustrating K_{asym} dependence on ΔV_{jh} measured in seven HeLaCx45/HeLaCx43-EGFP cell pairs when either the Cx43-EGFP cell (solid circles) or the Cx45 cell (open circles) was pulsed. ΔV_{jh} strongly affected electrical cou-

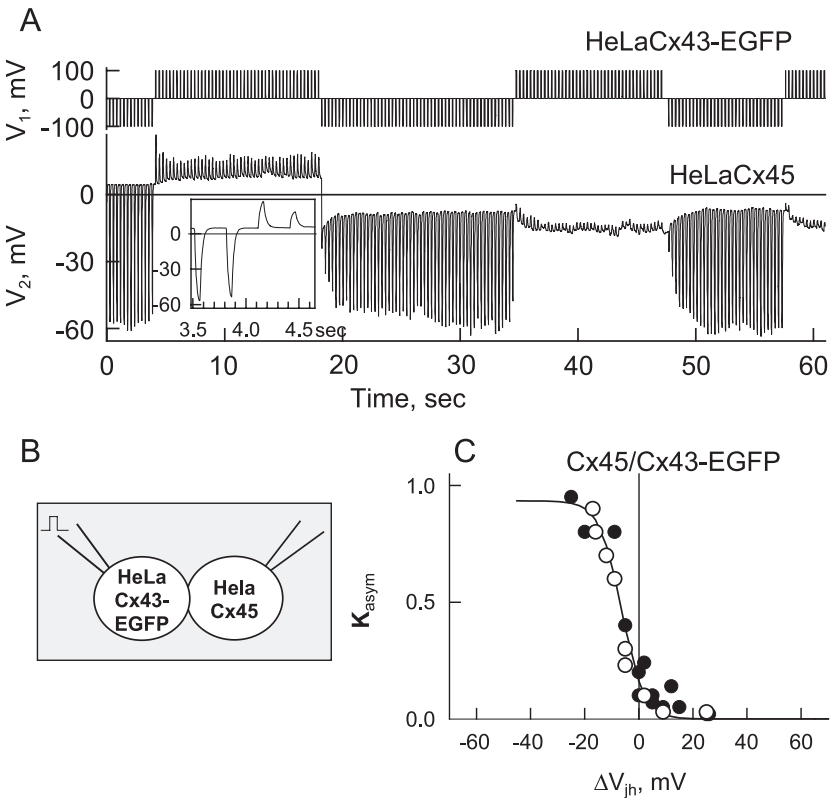

Fig. 10. Asymmetry of electrical coupling mediated by heterotypic Cx45/Cx43-EGFP junctions. (A) The HeLaCx43-EGFP cell (V_1) was voltage-clamped to positive or negative 100-mV, 30-ms rectangular pulses at 3 Hz from a holding potential of 0 mV. The HeLaCx45 cell (V_2) was current-clamped, and the steady-state holding potential was varied from ~ 5 mV (0–20 s) to ~ − 8 mV (20–62 s). Electrical coupling was much greater for negative pulses and coupling asymmetry increased by making the Cx45 side more negative. (B) Schematic of a cell pair; voltage steps were applied to HelaCx43-EGFP cell. (C) Pooled data of the electrical coupling asymmetry coefficient, K_{asym}, vs. ΔV_{jh} measured in seven Cx45/Cx43-EGFP cell pairs. Filled and open circles correspond to experiments in which the Cx43-EGFP or Cx45 cell was voltage-clamped and stepped, respectively. Solid line shows data fit to sigmoid function, $K_{asym} = A/(1 + \exp(b(\Delta V_{jh} - \Delta V_{jho})))$, with parameters $A = 0.9338$, $b = 0.24$ mV^{-1}, $\Delta V_{jho} = -6.4$ mV. Adapted from Ref. [76].

pling asymmetry. K_{asym} varied from near 1 (almost no asymmetry) when the Cx45 cell was more positive and close to 0 (maximal asymmetry) when the Cx45 cell was more negative.

In summary, these data in conjunction with gating properties of Cx45/Cx43-EGFP junctions shown in Fig. 9 demonstrate that asymmetry of electrical coupling largely is due to the slow gating mechanism of Cx45 (for more details see Ref. [76]). Moreover, in response to voltage steps comparable in amplitude to action potentials, the slow gate can operate relatively quickly. It is important to point out that small variations in ΔV_{jh} of ± 10 mV around zero very effectively modulate the degree of asymmetry and at $\Delta V_{jh} = \sim 10–15$ mV positive on the Cx43-EGFP side, electrical coupling is almost unidirectional. Thus, a synapse with Cx45 on the presynaptic side and Cx43 on the postsynaptic side could be highly rectifying. We also observed markedly asymmetric electrical signaling in Cx45/Cx47 and Cx45/Cx31 heterotypic junctions (our unpublished data). Electrical transmission at synapses using this mechanism would differ from known electrical synapses that are involved in escape systems, where the rectification is very rapid (~ 0.1 ms, [79–81]), and presumably is due to single channel rectification as seen in Cx26/Cx32 junctions [48,57]. It is interesting that all rectifying electrical synapses examined thus far demonstrate that the presynaptic side is more hyperpolarized by ~ 10–15 mV compared to the postsynaptic side [82–84]. Fast rectification can further increase asymmetry of electrical signaling. Data from several laboratories have shown that heterotypic junctions possess fast and slow forms of rectification. Fast rectification is a property of open channel conductance and is virtually instantaneous [43,48,57,70,85,86]. Slow rectification is a property of V_j gating and is determined by differences in V_j gating sensitivities and polarities of component hemichannels [37,40,67,87,88]. Both forms of rectification determine asymmetry of transjunctional signaling that, in extreme cases, can be unidirectional [76].

Rectifying heterotypic junctions similar to Cx45/Cx43 is possible between oligodendrocytes and astrocytes [89], Schwann cells and fibroblasts [77], and cells of the conductive system of the heart and atrial and ventricular myocytes [90]. Cardiac action potentials are long enough to alter coupling at the asymmetric junctions, and may play a role in coupling asymmetry between cells of conductive and working myocardium.

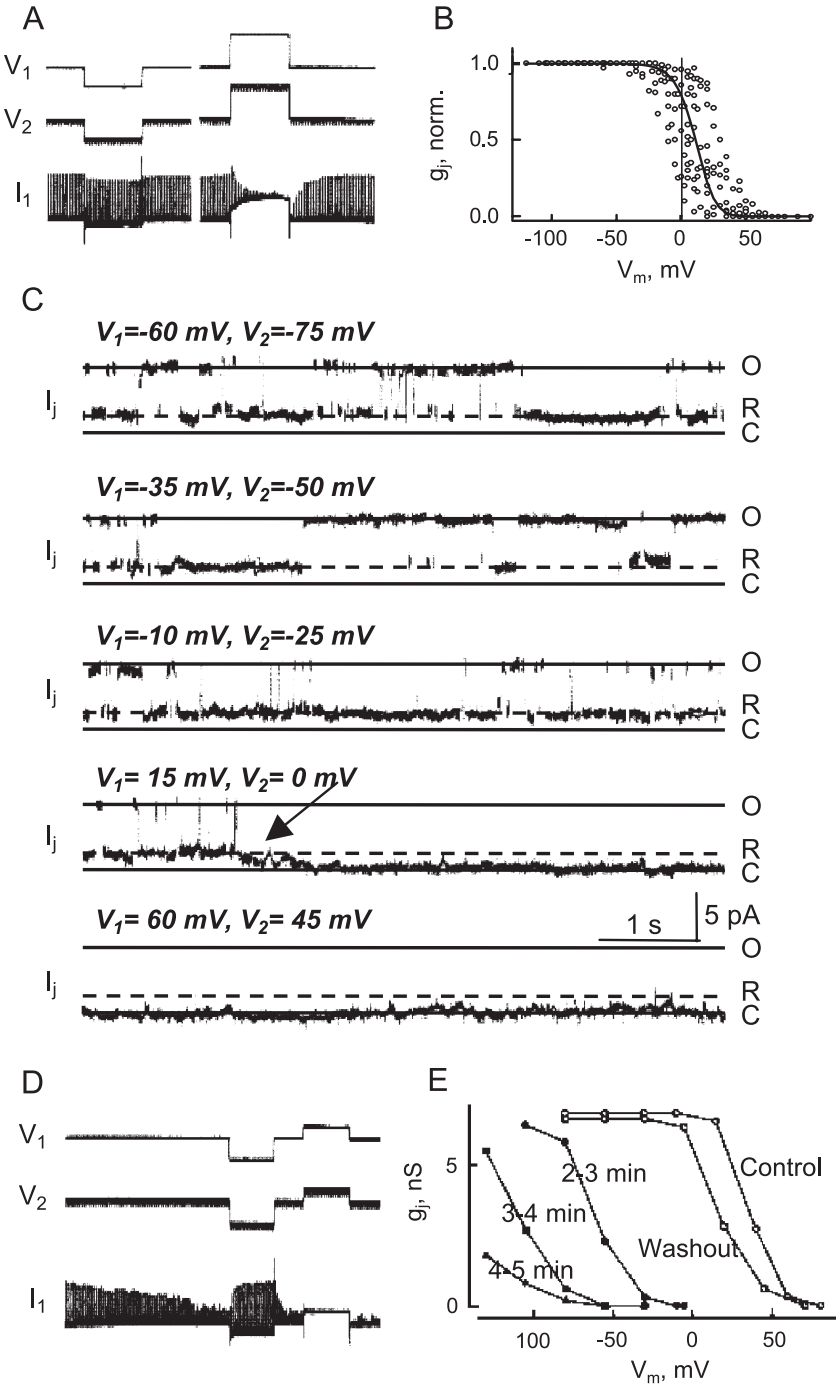

Fig. 11. V_m and chemical gating in C6/9 cell pairs. (A) Shown is an example of V_m gating. Both cells were clamped to the same V_m (-35 mV) and a test pulse of 15 mV was applied repeatedly (1 Hz) to cell 2 to assay I_j (upward deflections in current record of cell 1, I_1). A hyperpolarizing step of -50 mV has no effect on I_j, while the depolarizing step of $+80$ mV produces a reversible decrease in g_j down to ~ 0. (B) Summarized g_j-V_j plot (normalized) measured in eight cell pairs. The continuous curve is a fit of the data to the Boltzmann equation. (C) Example of V_m dependence of g_j at the single channel level. Shown are I_j records obtained by using the double whole cell patch clamp method. V_m was imposed by applying equal and simultaneous polarizations to both cells. V_j was held constant throughout at -15 mV. At V_ms in cell 1 of -60, -35 and -10 mV, the channel gates between γ_{open}, indicated by level O, and γ_{res} (dashed line, R). Depolarization from -60 to -10 mV decreases the relative time spent in γ_{open}. Further depolarization to $+15$ mV causes the channel to close, indicated by level C. At $+60$ mV the channel resides only in closed state. The transition to closed state has an apparently slow time course and is ascribed to V_m gating. Transitions between γ_{open} and γ_{res} are rapid and are ascribed to V_j gating. (D–E) Effect of heptanol on the g_j-V_m relationship. (D) Exposure to 1 mM heptanol leads to a gradual decline in I_j. A conditioning pulse from -35 to -85 mV increases I_j, while a conditioning pulse to -10 mV led to complete uncoupling. (E) Time course of g_j-V_m dependencies measured at different time intervals of C6/36 cell pair treatment with heptanol. V_m gating was measured under control perfusion (open circles) and 2–3 (filled circles), 3–4 (filled squares) and 4–5 min (filled triangles) under heptanol perfusion. Washout from heptanol returns the g_j-V_m curve close to that obtained under control conditions. Adapted from [46,52].

2.2. V_m-sensitive gating

Sensitivity to V_j is widespread among GJs in vertebrates and invertebrates, whereas sensitivity to V_m is less frequent in vertebrates. V_m dependence was first described in *Chironomus* salivary glands [10]. Equal and simultaneous hyperpolarization of both cells caused g_j to increase to a maximum, whereas depolarization caused g_j to decrease virtually to zero. Subsequently it was shown that junctions in salivary glands of the fruit fly *Drosophila melanogaster* [11] and insect cell lines of *A. albopictus* (clone C6/36) [12] and *Spodaptera frugiperda* (clone Sf9) [74] showed a sigmoidal g_j-V_m relation that exhibited a strong decrease in g_j with depolarization of both cells of a cell pair (see Fig. 11A and B). Unlike reported in *Chironomus*, GJs in *D. melanogaster, A. albopictus* and *S. frugiperda* also exhibit V_j dependence.

Evidence suggesting that V_m dependence differs mechanistically from V_j dependence comes from single channel studies in *Aedes* cells [46]. Shown in Fig. 11C are records from an *Aedes* cell pair in which there appeared to be only one active channel. With an imposed V_j, the channel gates mainly between the γ_{open} and γ_{res}. However, if the same V_j is maintained and both cells depolarized equally, then transitions to a fully closed state increase in frequency. Residence times in the closed state are prolonged with further depolarization of both cells, indicating that the transitions associated with closed state are due to V_m. The transitions between γ_{open} or γ_{res} and the closed state are slow and unlike the fast transitions associated with the fast V_j gating mechanism. This behavior is very similar to that observed during chemical gating [52] and in Cx46 hemichannels at inside negative voltages [26]. The resemblance of these 'slow' or multistep current transitions to the 'formation' currents observed during de novo channel opening [46] suggests that these gating mechanisms may be related and may represent conformational changes associated with the extracellular loops of the connexins. The differences in the steady-state and kinetic properties of gating by V_m and V_j suggest that they induce activation of different gating mechanisms. However, there appears to be an interaction between these two voltage gating mechanisms, because the dwell times in γ_{open} and γ_{res}, at the same V_j, change with V_m [11]. Even more evident is an interaction between V_m and chemical gating. In cells demonstrating strong V_m dependence, uncoupling by the potent chemical uncouplers, such as long-chain alkanols, arachidonic acid, low pH_i, and high $[Ca^{2+}]_i$, can be enhanced or rescued by depolarizing or hyperpolarizing V_ms, respectively (Fig. 11D and E; see also Refs. [10,52]). These data suggest that chemical- and voltage-sensitive slow gating mechanisms interact and may share common structural elements.

V_m dependence is also a property of GJs formed of some connexins. GJ channels formed of Cx57 [91] and Cx45 [92] demonstrate g_j-V_m dependence but to a less extent than GJs of invertebrates. We examined V_m gating in Cx47 and Cx47-EGFP as well as Cx43 and Cx43-EGFP GJs expressed in HeLa cells and none of them exhibited measurable V_m dependence. Presumably, the extent of V_m gating varies among different Cxs as well as expression systems, i.e., Cx43 expressed in *Xenopus* oocytes shows quite well expressed V_m sensitivity [93].

3. Chemical gating

Chemical agents that reduce coupling usually do not leave a residual conductance and their effect is readily reversible. Chemical gating can also include indirect action of a chemical agent via an intermediary that modifies the channel leading to gating. Evolutionary aspects of chemical gating mechanisms are presented in detail in Dr. Peracchia's article of this issue. There are a number of chemical agents that uncouple cells completely, such as long-chain alkanols, local anesthetics, acidifiers and, more recently, glycerrhetinic acid derivatives and quinine (for reviews see Ref. [9]). Low pH closes most GJ channels and may serve as a mechanism to limit the spread of injury from damaged to normal tissue. It was shown that low pH produces full uncoupling of Cx43 and Cx45 GJ channels by inducing slow gating transitions between open and closed states [50,94]. All GJ channels display chemical gating, which shares several features in common with slow V_j- or V_m-sensitive gating, i.e., g_j is reduced to zero and channels close fully with slow, stepwise transitions. The slow kinetics of the chemical gate may reflect complex conformational changes that require the participation of all six connexins of a hemichannel (connexon) or all 12 connexins of the full cell–cell channel. The gating activity of individual connexins is probably fast, but may not always be synchronous and this may result in the appearance that transitions between open and closed states are slow or consist of a series of resolvable transient sub-transitions.

Do we know anything about the molecular mechanisms of any of the chemical uncouplers? The most studied mechanism of chemical uncoupling is the one that occurs by cytoplasmic acidification. In Trexler et al. [95], we used fast solution switching (~ 1 ms) to demonstrate that pH acts directly on hemichannels rather than indirectly through soluble intermediates. Studies of channels and unapposed hemichannels exhibited two effects of low cytoplasmic pH. Short exposures to a low cytoplasmic pH produce rapid and completely reversible reductions in conductance. Longer acidifications lead to reduced g_j and to complete recovery [95]. Hemichannel studies with a rapid application of low pH showed that the onset of the decrease in current with acidification has no detectable latency consistent with direct action of protons on the connexin (Fig. 12A), most likely by direct titration of His or Cys residues. Longer low pH exposures produced increasingly incomplete recoveries [95]. These data support direct action of H^+ on the connexin itself. It may be that initial titration of a residue leads to a

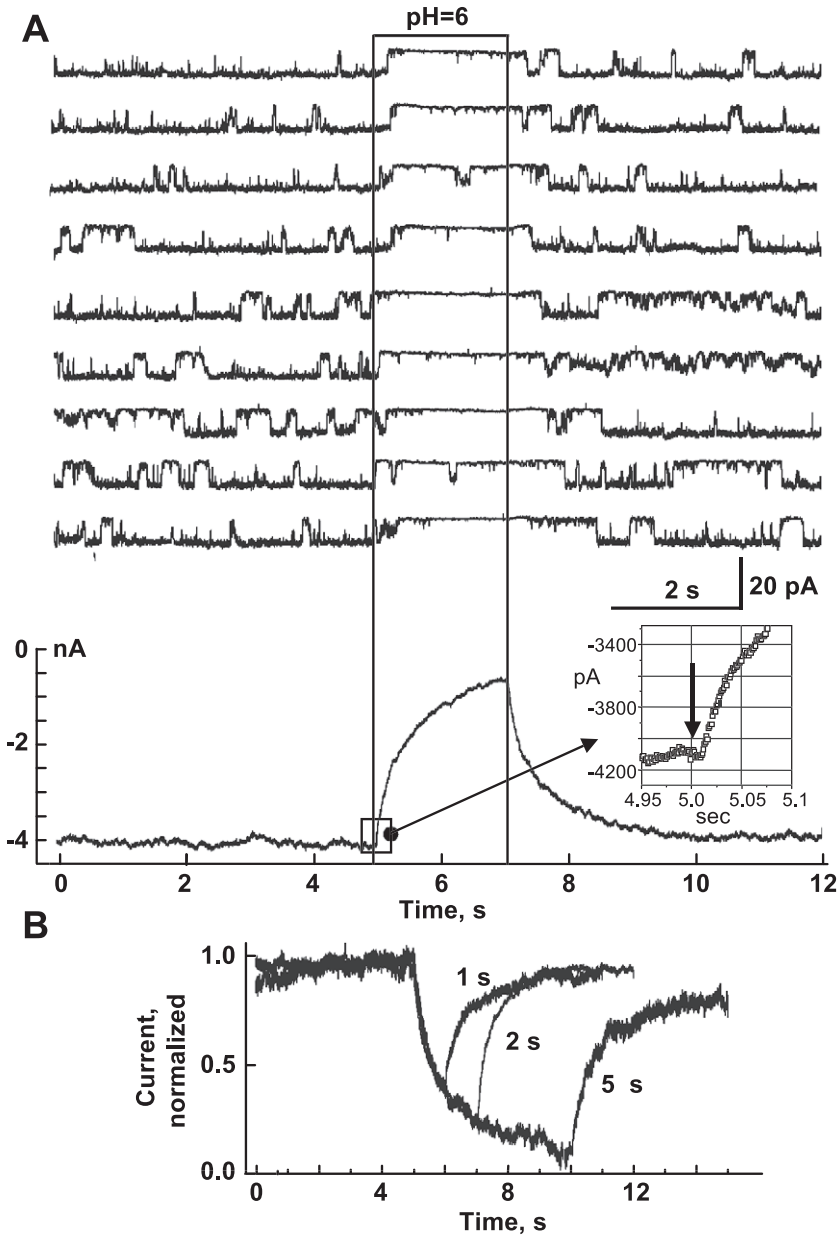

Fig. 12. Rapid effect of pH-induced closure in hemichannels indicates direct action of H^+ on connexins. (A) An inside-out patch containing a single Cx46 hemichannel was subjected to repeated applications of pH 6.0 (region within the rectangle). Membrane potential was held at − 30 mV; hemichannel openings are downward deflections in current. Summation of similar currents from >100 traces obtained from a total of five separate patches shows no measurable delay between pH 6.0 application and the decrease in current. (B) Ensemble currents show a second effect of pH that is sensitive to the duration of acidification. Ensemble currents from multiple patches were normalized to the average prior to acidification. Recovery from 1- and 2-s applications was nearly 100%, whereas recovery from 5-s applications was only ~ 80%. Longer exposures further reduced degree of recovery. The same phenomenon was observed in cell–cell channels. Adapted from Ref. [95].

closed conformation, i.e., gating, that exposes secondary sites, which by acting with slow kinetics lead to a "closed" conformation that is locked. The H^+ binding that initiates the gating effect of pH was deduced to be on the cytoplasmic side of the hemichannel, presumably near the entrance to the pore [95]. Several studies of cell–cell channels performed in *Xenopus* oocytes have proposed involvement of residues in the CL and carboxy terminus in the pH gating [96–99]. The carboxy terminus has been proposed to behave like a gating particle that, when titrated, binds to a receptor domain that leads to channel closure [100]. Wang et al. [101] demonstrated that replacing CL of Cx32 with CL of Cx38 increased pH-gating sensitivity to that of Cx38 channels, suggesting that CL is important in pH-sensitive gating. Although it was shown that much of the CT of Cx32 is irrelevant for pH gating because deletion of ~ 85% of CT does not affect kinetics of an uncoupling, the initial segment of CT significantly modulated pH gating sensitivity

of Cx32 channels [102,103]. Replacing five positively charged arginines (R215, R219, R220, R223 and R224) either with polar residues (N or T), histidine (H) or glutamic acid (E) greatly increased the sensitivity of Cx32 channels to intracellular acidification induced by application of CO_2. Interestingly, the initial segment of CT has been identified as a CaM binding domain [104] and its basic residues would be expected to be relevant for interaction with CaM, which can plug the channel mouth [56].

Since the longer-term mechanisms of closure of gap channels by chemical agents may involve perturbation of inter-channel and/or lipid–connexin interactions [105], use of GFP-tagged connexins has been useful in examining whether prolonged exposure to uncoupling agents causes measurable changes in fluorescence intensity or in the size and shape of junctional plaques. Thus far, exposure to acidification, alkanols or anesthetics under conditions that cause uncoupling has not shown disruption of plaques or any gross changes in fluorescence distribution visible by fluorescence microscopy [51]. These results indicate that chemical uncoupling, even when long-term and not readily reversible, does not act by dispersing channels within a plaque or by gross disruption of packing.

4. Summary

A schematic presentation of our current view of gating mechanisms of GJ channels is illustrated in Fig. 13. GJ channels contain fast and slow gates, both of which are sensitive to V_j [51]. The fast V_j gate (arrows with circle) exhibits fast gating transitions (~ 1 ms) to the residual state, and the slow V_j gate (arrows with square) exhibits slow gating transitions (~ 10 ms) to the fully closed state. The finding that single amino acid mutations in N-terminus can reverse gating polarity of the fast V_j gating mechanism without affecting the behavior of the slow V_j gating mechanism [55], as well as a loss of the fast V_j gating in Cx43-Aequorin and Cx43-GFP fusion proteins [32,68] or after deletion of CT [42,106], provides evidence that fast and slow V_j gating mechanisms are molecularly distinct. These data suggest that the fast V_j gate is located at the cytoplasmic entrance of hemichannels. In addition, current flowing through open Cx32 and Cx43 channels is linear with V_j, but rectifies when these channels are in the residual state [57,62]. Rectification could be explained by narrowing of the cytoplasmic entrance that effectively increases the electrostatic influence of positive charges located there [57]. Mutations of a proline in TM2 conserved among all connexins were shown to strongly affect V_j gating [107], and in Cx32 this proline was shown to behave in a manner consistent with a proline kink motif [66]. The conformational changes in TM2 may, in turn, cause narrowing at the cytoplasmic ends of the channel. Fast V_j gating to the residual state in Cx43 channel makes the pore more anion-selective and appears to cause significant narrowing as evidenced by a substantial decrease in unitary conductance and a reduction in the cutoff size for permeant dye molecules [62,65].

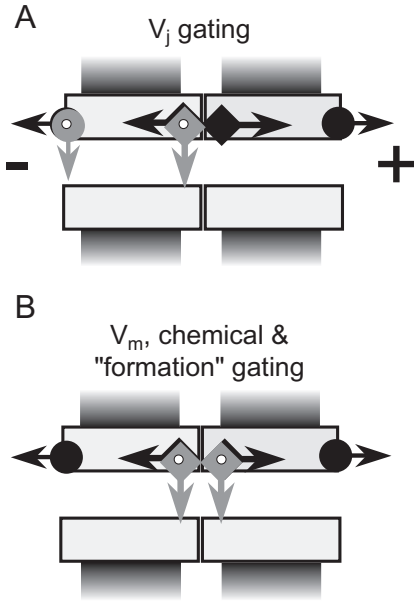

Fig. 13. Schematics of a Cx43 gap junction channel containing fast (arrow with circle) and slow (arrow with square) gates. (A) V_j initiates gating mediated by both fast and slow gating mechanisms. (B) V_m and chemical uncouplers initiate gating mediated by the slow gating mechanism in both hemichannels. Gating transitions measured during the first channel opening during de novo channel formation are also slow and stepwise resembling gating transitions induced by V_m and chemical uncouplers.

The slow V_j or 'loop' gate as well as the gate(s) operated by chemical uncoupling agents all exhibit slow gating transitions and may represent one in the same gate. Such a putative 'common gate' may be located towards the center of a cell–cell channel, or towards the extracellular end of an unapposed hemichannel. Pfahnl and Dahl [108], based on cysteine scanning studies, suggested that in Cx46 hemichannels the 'loop' gate is located extracellular to position L35, which is in TM2. We suggest that this common slow gating element can be triggered by different sensorial elements located in different regions of the connexin. This hypothesis is supported by data showing that uncoupling induced by long-chain alkanols, arachidonic acid, high $[Ca^{2+}]_i$, or $[H^+]_i$ can be reversed by hyperpolarization in cells that demonstrate V_m-sensitive gating [10,52].

During the last several years, the two gating mechanism hypothesis has received support from studies of a number of different Cxs performed in different laboratories [42,43,54,55,109,110]. It is now evident that not only cell–cell channels but also unapposed hemichannels contain two gating mechanisms [26,55]. The two gating mechanisms interact in a manner consistent with contingent gating of two series gates in each hemichannel. Although experimental data can be explained having two distinct gates interacting through their effect on the electric field inside the channel, it cannot rule out interactions that may occur

through an allosteric mechanism or through sharing of molecular components.

GJ channels formed from different Cx isoforms vary considerably in single channel conductance, selectivity, sensitivity to V_j and chemical gating. Theoretically, hundreds of heterotypic and thousands of heteromeric GJ channel types can be formed in organ-systems within a Cx family that contains over 20 isoforms [8]. In practice, it is impossible to examine functional properties all of them. However, knowing the basic functional properties of homotypic junctions and how they interact in assembled heterotypic or heteromeric channels are important in elucidating their potential functional roles. Studies of the Cx43/Cx45 heterotypic junction provide a good example. This junction can explain signal transfer asymmetry, rectification, unidirectional signal transmission in electrical synapses and, even retrospectively, a functional significance for the long-known fact that there are differences in resting potentials between pre- and postsynaptic structures at rectifying electrical synapses [82–84]. To make future progress in our understanding of how heterotypic–heteromeric junctions function, it is important to determine the gating polarities of both fast and slow gates as well as the rectification of $I–V$ relations of open and residual states. Very little is known about metabolic communication or chemical signaling through heterotypic channels and even less through heteromeric channels. It would be important to determine whether metabolic communication and chemical signaling through heterotypic channels also can be modulated by ΔV_{jh}. This would provide a role for V_j gating in inexcitable cells, which presumably do not utilize electrical signaling.

Acknowledgements

We would like to thank all our collaborators and co-authors in the papers that were employed in this review and specifically to: Dr. T.A. Bargiello, Dr. M.V.L. Bennett, Dr. A. Bukauskiene, Dr. D. Laird, Dr. S. Oh, Dr. C. Peracchia, Dr. E.B. Trexler, Dr. R. Weingart, Dr. K. Willecke. This work was supported by NIH Grants: NS36706 to F.F.B. and GM54179 to V.K.V.

References

[1] M.V. Bennett, Connexins in disease [news], Nature 368 (1994) 18–19.
[2] C. Elfgang, R. Eckert, H. Lichtenberg-Frate, A. Butterweck, O. Traub, R.A. Klein, D.F. Hulser, K. Willecke, Specific permeability and selective formation of gap junction channels in connexin-transfected HeLa cells, J. Cell Biol. 129 (1995) 805–817.
[3] D.A. Goodenough, J.A. Goliger, D.L. Paul, Connexins, connexons, and intercellular communication, Annu. Rev. Biochem. 65 (1996) 475–502.
[4] D.L. Paul, Molecular cloning of cDNA for rat liver gap junction protein, J. Cell Biol. 103 (1986) 123–134.
[5] E.L. Hertzberg, R.M. Disher, A.A. Tiller, Y. Zhou, R.G. Cook, Topology of the Mr 27,000 liver gap junction protein. Cytoplasmic localization of amino- and carboxyl termini and a hydrophilic domain which is protease-hypersensitive, J. Biol. Chem. 263 (1988) 19105–19111.
[6] S.B. Yancey, S.A. John, R. Lal, B.J. Austin, J.P. Revel, The 43-kD polypeptide of heart gap junctions: immunolocalization, topology, and functional domains, J. Cell Biol. 108 (1989) 2241–2254.
[7] M. Yeager, V.M. Unger, M.M. Falk, Synthesis, assembly and structure of gap junction intercellular channels, Curr. Opin. Struct. Biol. 8 (4) (1998) 517–524.
[8] K. Willecke, J. Eiberger, J. Degen, D. Eckardt, A. Romualdi, M. Guldenagel, U. Deutsch, G. Sohl, Structural and functional diversity of connexin genes in the mouse and human genome, Biol. Chem. 383 (2002) 725–737.
[9] A.L. Harris, Emerging issues of connexin channels: biophysics fills the gap, Q. Rev. Biophys. 34 (2001) 325–427.
[10] A.L. Obaid, S.J. Socolar, B. Rose, Cell-to-cell channels with two independent regulated gates in series: analysis of junctional channel modulation by membrane potential, calcium and pH, J. Membr. Biol. 73 (1983) 69–89.
[11] V.K. Verselis, M.V. Bennett, T.A. Bargiello, A voltage-dependent gap junction in *Drosophila melanogaster*, Biophys. J. 59 (1991) 114–126.
[12] F. Bukauskas, C. Kempf, R. Weingart, Electrical coupling between cells of the insect *Aedes albopictus*, J. Physiol. 448 (1992) 321–337.
[13] P. Phelan, T.A. Starich, Innexins get into the gap, BioEssays 23 (5) (2001) 388–396.
[14] Y. Panchin, I. Kelmanson, M. Matz, K. Lukyanov, N. Usman, S. Lukyanov, A ubiquitous family of putative gap junction molecules, Curr. Biol. 29 (2000) R473–R474.
[15] R. Bruzzone, S.G. Hormuzdi, M.T. Barbe, A. Herb, H. Monyer, Pannexins, a family of gap junction proteins expressed in brain, Proc. Natl. Acad. Sci. U.S.A. 100 (2003) 13644–13649.
[16] I.V. Kelmanson, D.A. Shagin, N. Usman, M.V. Matz, S.A. Lukyanov, Y.V. Panchin, Altering electrical connections in the nervous system of the pteropod mollusc *Clione limacina* by neuronal injections of gap junction mRNA, Eur. J. Neurosci. 16 (2002) 2475–2476.
[17] L.S. Musil, D.A. Goodenough, Multisubunit assembly of an integral plasma membrane channel protein, gap junction connexin43, occurs after exit from the ER, Cell 74 (1993) 1065–1077.
[18] S. Rahman, G. Carlile, W.H. Evans, Assembly of hepatic gap junctions. Topography and distribution of connexin 32 in intracellular and plasma membranes determined using sequence-specific antibodies, J. Biol. Chem. 268 (1993) 1260–1265.
[19] C.H. George, J.M. Kendall, W.H. Evans, Intracellular trafficking pathways in the assembly of connexins into gap junctions, J. Biol. Chem. 274 (13) (1999) 8678–8685.
[20] J.A. Diez, S. Ahmad, W.H. Evans, Assembly of heteromeric connexons in guinea-pig liver en route to the Golgi apparatus, plasma membrane and gap junctions, Eur. J. Biochem. 262 (1) (1999) 142–148.
[21] G.A. Zampighi, D.D. Loo, M. Kreman, S. Eskandari, E.M. Wright, Functional and morphological correlates of connexin50 expressed in Xenopus laevis oocytes, J. Gen. Physiol. 113 (4) (1999) 507–524.
[22] P.E. Martin, G. Blundell, S. Ahmad, R.J. Errington, W.H. Evans, Multiple pathways in the trafficking and assembly of connexin 26, 32 and 43 into gap junction intercellular communication channels, J. Cell. Sci. 114 (Pt 21) (2001) 3845–3855.
[23] J. Das Sarma, R.A. Meyer, F. Wang, V. Abraham, C.W. Lo, M. Koval, Multimeric connexin interactions prior to the trans-Golgi network, J. Cell. Sci. 114 (Pt 22) (2001) 4013–4024.
[24] G. Gaietta, T.J. Deerinck, S.R. Adams, J. Bouwer, O. Tour, D.W. Laird, G.E. Sosinsky, R.Y. Tsien, M.H. Ellisman, Multicolor and electron microscopic imaging of connexin trafficking, Science 296 (2002) 503–507.

[25] L. Ebihara, E. Steiner, Properties of a nonjunctional current expressed from a rat connexin46 cDNA in Xenopus oocytes, J. Gen. Physiol. 102 (1993) 59–74.
[26] E.B. Trexler, M.V. Bennett, T.A. Bargiello, V.K. Verselis, Voltage gating and permeation in a gap junction hemichannel, Proc. Natl. Acad. Sci. U. S. A. 93 (1996) 5836–5841.
[27] R. Johnson, M. Hammer, J. Sheridan, J.P. Revel, Gap junction formation between reaggregated Novikoff hepatoma cells, Proc. Natl. Acad. Sci. U. S. A. 71 (1974) 4536–4540.
[28] P.D. Lampe, W.E. Kurata, B.J. Warn-Cramer, A.F. Lau, Formation of a distinct connexin43 phosphoisoform in mitotic cells is dependent upon p34cdc2 kinase, J. Cell. Sci. 111 (Pt 6) (1998) 833–841.
[29] P.D. Lampe, Q. Qiu, R.A. Meyer, E.M. TenBroek, T.F. Walseth, T.A. Starich, H.L. Grunenwald, R.G. Johnson, Gap junction assembly: PTX-sensitive G proteins regulate the distribution of connexin43 within cells, Am. J. Physiol., Cell Physiol. 281 (4) (2001) C1211–C1222.
[30] M.M. Falk, Connexin-specific distribution within gap junctions revealed in living cells, J. Cell. Sci. 113 (Pt 22) (2000) 4109–4120.
[31] K. Jordan, J.L. Solan, M. Dominguez, M. Sia, A. Hand, P.D. Lampe, D.W. Laird, Trafficking, assembly, and function of a connexin43-green fluorescent protein chimera in live mammalian cells, Mol. Biol. Cell 10 (6) (1999) 2033–2050.
[32] F.F. Bukauskas, K. Jordan, A. Bukauskiene, M.V. Bennett, P.D. Lampe, D.W. Laird, V.K. Verselis, Clustering of connexin 43-enhanced green fluorescent protein gap junction channels and functional coupling in living cells, Proc. Natl. Acad. Sci. U. S. A. 97 (6) (2000) 2556–2561.
[33] A.L. Harris, D.C. Spray, M.V. Bennett, Kinetic properties of a voltage-dependent junctional conductance, J. Gen. Physiol. 77 (1981) 95–117.
[34] D.C. Spray, A.L. Harris, M.V. Bennett, Equilibrium properties of a voltage-dependent junctional conductance, J. Gen. Physiol. 77 (1981) 77–93.
[35] V.K. Verselis, R.D. Veenstra, Gap junction channels. Permeability and voltage gating, in: E. Hertzberg (Ed.), Advances in Molecular and Cell Biology, vol. 30. JAI Press, Stamford, CT, 2000, pp. 129–192.
[36] A.P. Moreno, M.B. Rook, G.I. Fishman, D.C. Spray, Gap junction channels: distinct voltage-sensitive and -insensitive conductance states, Biophys. J. 67 (1994) 113–119.
[37] R. Werner, E. Levine, C. Rabadan Diehl, G. Dahl, Formation of hybrid cell–cell channels, Proc. Natl. Acad. Sci. U. S. A. 86 (1989) 5380–5384.
[38] K. Willecke, H. Hennemann, E. Dahl, S. Jungbluth, R. Heynkes, The diversity of connexin genes encoding gap junctional proteins, Eur. J. Cell Biol. 56 (1991) 1–7.
[39] M.B. Rook, A.C. van Ginneken, B. de Jonge, A. el Aoumari, D. Gros, H.J. Jongsma, Differences in gap junction channels between cardiac myocytes, fibroblasts, and heterologous pairs, Am. J. Physiol. 263 (1992) C959–C977.
[40] T.W. White, D.L. Paul, D.A. Goodenough, R. Bruzzone, Functional analysis of selective interactions among rodent connexins, Mol. Biol. Cell 6 (1995) 459–470.
[41] E. Steiner, L. Ebihara, Functional characterization of canine connexin45, J. Membr. Biol. 150 (1996) 153–161.
[42] A. Revilla, C. Castro, L.C. Barrio, Molecular dissection of transjunctional voltage dependence in the connexin-32 and connexin-43 junctions, Biophys. J. 77 (3) (1999) 1374–1383.
[43] S. Elenes, A.D. Martinez, M. Delmar, E.C. Beyer, A.P. Moreno, Heterotypic docking of Cx43 and Cx45 connexons blocks fast voltage gating of Cx43, Biophys. J. 81 (3) (2001) 1406–1418.
[44] F.F. Bukauskas, R. Weingart, Multiple conductance states of newly formed single gap junction channels between insect cells, Pflugers Arch. 423 (1993) 152–154.
[45] R. Weingart, F.F. Bukauskas, Gap junction channels of insects exhibit a residual conductance, Pflugers Arch. 424 (1993) 192–194.
[46] F.F. Bukauskas, R. Weingart, Voltage-dependent gating of single gap junction channels in an insect cell line, Biophys. J. 67 (1994) 613–625.
[47] F.F. Bukauskas, C. Elfgang, K. Willecke, R. Weingart, Biophysical properties of gap junction channels formed by mouse connexin40 in induced pairs of transfected human HeLa cells, Biophys. J. 68 (1995) 2289–2298.
[48] F.F. Bukauskas, C. Elfgang, K. Willecke, R. Weingart, Heterotypic gap junction channels (connexin26–connexin32) violate the paradigm of unitary conductance, Pflugers Arch. 429 (1995) 870–872.
[49] V. Valiunas, F.F. Bukauskas, R. Weingart, Conductances and selective permeability of connexin43 gap junction channels examined in neonatal rat heart cells, Circ. Res. 80 (5) (1997) 708–719.
[50] F.F. Bukauskas, C. Peracchia, Two distinct gating mechanisms in gap junction channels: CO_2-sensitive and voltage-sensitive, Biophys. J. 72 (5) (1997) 2137–2142.
[51] F.F. Bukauskas, A. Bukauskiene, M.V. Bennett, V.K. Verselis, Gating properties of gap junction channels assembled from connexin43 and connexin43 fused with green fluorescent protein, Biophys. J. 81 (1) (2001) 137–152.
[52] R. Weingart, F.F. Bukauskas, Long-chain n-alkanols and arachidonic acid interfere with the V_m-sensitive gating mechanism of gap junction channels, Pflugers Arch. 435 (2) (1998) 310–319.
[53] G. Schmilinsky-Fluri, V. Valiunas, M. Willi, R. Weingart, Modulation of cardiac gap junctions: the mode of action of arachidonic acid, J. Mol. Cell. Cardiol. 29 (6) (1997) 1703–1713.
[54] K. Banach, R. Weingart, Voltage gating of Cx43 gap junction channels involves fast and slow current transitions, Pflugers Arch. 439 (3) (2000) 248–250.
[55] S. Oh, C.K. Abrams, V.K. Verselis, T.A. Bargiello, Stoichiometry of transjunctional voltage-gating polarity reversal by a negative charge substitution in the amino terminus of a connexin32 chimera [see comments], J. Gen. Physiol. 116 (1) (2000) 13–31.
[56] C. Peracchia, X.G. Wang, L.M. Peracchia, Behavior of chemical and slow voltage-gates of connexin channels—the "cork" gating hypothesis, in: C. Peracchia (Ed.), Gap Junctions—Molecular Basis of Cell Communication in Health and Disease, Academic Press, San Diego, CA, 2000, pp. 271–295.
[57] S. Oh, J.B. Rubin, M.V. Bennett, V.K. Verselis, T.A. Bargiello, Molecular determinants of electrical rectification of single channel conductance in gap junctions formed by connexins 26 and 32, J. Gen. Physiol. 114 (3) (1999) 339–364.
[58] D.M. Larson, R.J. Gilbert, E.C. Beyer, Two-dimensional coupling by gap junctions in cultured gastric smooth muscle monolayers, Am. J. Physiol. 263 (1992) G261–G268.
[59] T.H. Steinberg, R. Civitelli, S.T. Geist, A.J. Robertson, E. Hick, R.D. Veenstra, H.Z. Wang, P.M. Warlow, E.M. Westphale, J.G. Laing, et al., Connexin43 and connexin45 form gap junctions with different molecular permeabilities in osteoblastic cells, EMBO J. 13 (1994) 744–750.
[60] R.D. Veenstra, H.Z. Wang, D.A. Beblo, M.G. Chilton, A.L. Harris, E.C. Beyer, P.R. Brink, Selectivity of connexin-specific gap junctions does not correlate with channel conductance, Circ. Res. 77 (1995) 1156–1165.
[61] V.K. Verselis, E.B. Trexler, F.F. Bukauskas, Connexin hemichannels and cell–cell channels: comparison of properties, Braz. J. Med. Biol. Res. 33 (4) (2000) 379–389.
[62] F.F. Bukauskas, A. Bukauskiene, V.K. Verselis, Conductance and permeability of the residual state of connexin43 gap junction channels, J. Gen. Physiol. 119 (2002) 171–186.
[63] D. Chen, J. Lear, B. Eisenberg, Permeation through an open channel: Poisson–Nerst–Planck theary of a synthetic ionic channel, Biophys. J. 72 (1997) 97–116.
[64] E.B. Trexler, F.F. Bukauskas, J. Kronengold, T.A. Bargiello, V.K. Verselis, The first extracellular loop domain is a major determinant of charge selectivity in connexin46 channels, Biophys. J. 79 (6) (2000) 3036–3051.

[65] Y. Qu, G. Dahl, Function of the voltage gate of gap junction channels: selective exclusion of molecules, Proc. Natl. Acad. Sci. U. S. A. 99 (2002) 697–702.
[66] Y. Ri, J.A. Ballesteros, C.K. Abrams, S. Oh, V.K. Verselis, H. Weinstein, T.A. Bargiello, The role of a conserved proline residue in mediating conformational changes associated with voltage gating of Cx32 gap junctions, Biophys. J. 76 (6) (1999) 2887–2898.
[67] V.K. Verselis, C.S. Ginter, T.A. Bargiello, Opposite voltage gating polarities of two closely related connexins, Nature 368 (1994) 348–351.
[68] P.E. Martin, C.H. George, C. Castro, J.M. Kendall, J. Capel, A.K. Campbell, A. Revilla, L.C. Barrio, W.H. Evans, Assembly of chimeric connexin-aequorin proteins into functional gap junction channels. Reporting intracellular and plasma membrane calcium environments, J. Biol. Chem. 273 (3) (1998) 1719–1726.
[69] L.C. Barrio, T. Suchyna, T. Bargiello, L.X. Xu, R.S. Roginski, M.V. Bennett, B.J. Nicholson, Gap junctions formed by connexins 26 and 32 alone and in combination are differently affected by applied voltage, Proc. Natl. Acad. Sci. U. S. A. 89 (1992) 4220.
[70] L.C. Barrio, T. Suchyna, T. Bargiello, L.X. Xu, R.S. Roginski, M.V. Bennett, B.J. Nicholson, Gap junctions formed by connexins 26 and 32 alone and in combination are differently affected by applied voltage, Proc. Natl. Acad. Sci. U. S. A. 88 (1991) 8410–8414.
[71] A.P. Moreno, G.I. Fishman, E.C. Beyer, D.C. Spray, Voltage dependent gating and single channel analysis of heterotypic gap junction channels formed of Cx45 and Cx43, in: Y.K.K. Kanno, Y. Shiba, Y. Shibata (Eds.), Intercellular Communication through Gap Junctions, Progress in Cell Research, vol. 4, Elsevier, Amsterdam, 1995, pp. 405–408.
[72] S. Haubrich, H.J. Schwarz, F. Bukauskas, H. Lichtenberg-Frate, O. Traub, R. Weingart, K. Willecke, Incompatibility of connexin 40 and 43 Hemichannels in gap junctions between mammalian cells is determined by intracellular domains, Mol. Biol. Cell 7 (12) (1996) 1995–2006.
[73] M.G. Hopperstad, M. Srinivas, D.C. Spray, Properties of gap junction channels formed by Cx46 alone and in combination with Cx50, Biophys. J. 79 (2000) 1954–1966.
[74] F.F. Bukauskas, R. Vogel, R. Weingart, Biophysical properties of heterotypic gap junctions newly formed between two types of insect cells, J. Physiol. (Lond.) 499 (Pt 3) (1997) 701–713.
[75] B.M. Altevogt, K.A. Kleopa, F.R. Postma, S.S. Scherer, D.L. Paul, Connexin29 is uniquely distributed within myelinating glial cells of the central and peripheral nervous systems, J. Neurosci. 22 (2002) 6458–6470.
[76] F.F. Bukauskas, A. Bukauskiene, V.K. Verselis, M.V.L. Bennett, Coupling asymmetry of heterotypic connexin 45/connexin 43-EGFP gap junctions: properties of fast and slow gating mechanisms, Proc. Natl. Acad. Sci. U. S. A. 99 (2002) 7113–7118.
[77] F. Bukauskas, P. Shrager, C. Peracchia, Gating Properties of Gap Junction Channels of Schwann Cells and Fibroblasts Isolated from the Sciatic Nerve of Neonatal Rats, IOS Press, Amsterdam, 1998.
[78] T.W. White, R. Bruzzone, D.A. Goodenough, D.L. Paul, Voltage gating of connexins [letter], Nature 371 (1994) 208–209.
[79] E.J. Furshpan, D.D. Potter, Transmission at the giant motor synapses of the crayfish, J. Physiol. (Lond.) 145 (1959) 289–325.
[80] A.A. Auerbach, M.V.L. Bennett, A rectifying electrotonic synapse in the central nervous system of a vertebrate, J. Gen. Physiol. 53 (1969) 211–237.
[81] S.W. Jaslove, P.R. Brink, The mechanism of rectification at the electrotonic motor giant synapse of the crayfish, Nature 323 (1986) 63–65.
[82] C. Giaume, R.T. Kado, H. Korn, Voltage-clamp analysis of a crayfish rectifying synapse, J. Physiol. (Lond.) 386 (1987) 91–112.
[83] W.J. Heitler, K. Fraser, D.H. Edwards, Different types of rectification at electrical synapses made by a single crayfish neurone investigated experimentally and by computer simulation, J. Comp. Physiol., A Sens. Neural Behav. Physiol 169 (1991) 707–718.
[84] A.E. Pereda, T.D. Bell, D.S. Faber, Retrograde synaptic communication via gap junctions coupling auditory afferents to the Mauthner cell, J. Neurosci. 15 (1995) 5943–5955.
[85] B.J. Nicholson, P.A. Weber, F. Cao, H. Chang, P. Lampe, G. Goldberg, The molecular basis of selective permeability of connexins is complex and includes both size and charge, Braz. J. Med. Biol. Res. 33 (4) (2000) 369–378.
[86] J.B. Rubin, V.K. Verselis, M.V. Bennett, T.A. Bargiello, Molecular analysis of voltage dependence of heterotypic gap junctions formed by connexins 26 and 32, Biophys. J. 62 (1992) 183–193 (discuss).
[87] H. Hennemann, T. Suchyna, H. Lichtenberg Frate, S. Jungbluth, E. Dahl, J. Schwarz, B.J. Nicholson, K. Willecke, Molecular cloning and functional expression of mouse connexin40, a second gap junction gene preferentially expressed in lung, J. Cell Biol. 117 (1992) 1299–1310.
[88] T.W. White, R. Bruzzone, S. Wolfram, D.L. Paul, D.A. Goodenough, Selective interactions among the multiple connexin proteins expressed in the vertebrate lens: the second extracellular domain is a determinant of compatibility between connexins, J. Cell Biol. 125 (1994) 879–892.
[89] J.E. Rash, T. Yasumura, F.E. Dudek, J.I. Nagy, Cell-specific expression of connexins and evidence of restricted gap junctional coupling between glial cells and between neurons, J. Neurosci. 21 (6) (2001) 1983–2000.
[90] H.V. van Rijen, T.A. van Veen, M.J. van Kempen, F.J. Wilms-Schopman, M. Potse, O. Krueger, K. Willecke, T. Opthof, H.J. Jongsma, J.M. de Bakker, Impaired conduction in the bundle branches of mouse hearts lacking the gap junction protein connexin40, Circulation 103 (11) (2001) 1591–1598.
[91] D. Manthey, F. Bukauskas, C.G. Lee, C.A. Kozak, K. Willecke, Molecular cloning and functional expression of the mouse gap junction gene connexin-57 in human HeLa cells, J. Biol. Chem. 274 (21) (1999) 14716–14723.
[92] L.C. Barrio, J. Capel, J.A. Jarillo, C. Castro, A. Revilla, Species-specific voltage-gating properties of connexin-45 junctions expressed in Xenopus oocytes, Biophys. J. 73 (2) (1997) 757–769.
[93] A. Revilla, M.V. Bennett, L.C. Barrio, Molecular determinants of membrane potential dependence in vertebrate gap junction channels, Proc. Natl. Acad. Sci. U. S. A. 97 (26) (2000) 14760–14765.
[94] F. Bukauskas, C. Peracchia, Distinct behaviors of chemical and voltage sensitive gates of gap junction channel, in: C. Peracchia (Ed.), Gap Junctions, vol. 49, Academic Press, San Diego, 2000, pp. 207–221.
[95] E.B. Trexler, F.F. Bukauskas, M.V. Bennett, T.A. Bargiello, V.K. Verselis, Rapid and direct effects of pH on connexins revealed by the connexin46 hemichannel preparation, J. Gen. Physiol. 113 (5) (1999) 721–742.
[96] J.F. Ek, M. Delmar, R. Perzova, S.M. Taffet, Role of histidine 95 on pH gating of the cardiac gap junction protein connexin43, Circ. Res. 74 (1994) 1058–1064.
[97] J.F. Ek-Vitorin, G. Calero, G.E. Morley, W. Coombs, S.M. Taffet, M. Delmar, PH regulation of connexin43: molecular analysis of the gating particle, Biophys. J. 71 (3) (1996) 1273–1284.
[98] X.G. Wang, C. Peracchia, Connexin 32/38 chimeras suggest a role for the second half of inner loop in gap junction gating by low pH, Am. J. Physiol. 271 (5 Pt 1) (1996) C1743–C1749.
[99] C. Peracchia, X.C. Wang, Connexin domains relevant to the chemical gating of gap junction channels, Braz. J. Med. Biol. Res. 30 (5) (1997) 577–590.
[100] D. Francis, K. Stergiopoulos, J.F. Ek-Vitorin, F.L. Cao, S.M. Taffet, M. Delmar, Connexin diversity and gap junction regulation by pHi, Dev. Genet. 24 (1–2) (1999) 123–136.
[101] X. Wang, L. Li, L.L. Peracchia, C. Peracchia, Chimeric evidence for a role of the connexin cytoplasmic loop in gap junction channel gating, Pflugers Arch. 431 (6) (1996) 844–852.

[102] X.G. Wang, C. Peracchia, Positive charges of the initial C-terminus domain of Cx32 inhibit gap junction gating sensitivity to CO_2, Biophys. J. 73 (2) (1997) 798–806.
[103] X.G. Wang, C. Peracchia, Molecular dissection of a basic COOH-terminal domain of Cx32 that inhibits gap junction gating sensitivity, Am. J. Physiol. 275 (5 Pt 1) (1998) C1384–C1390.
[104] K. Torok, K. Stauffer, W.H. Evans, Connexin 32 of gap junctions contains two cytoplasmic calmodulin-binding domains, Biochem. J. 326 (Pt 2) (1997) 479–483.
[105] J.M. Burt, K.D. Massey, B.N. Minnich, Uncoupling of cardiac cells by fatty acids: structure–activity relationships, Am. J. Physiol. 260 (1991) C439–C448.
[106] A.P. Moreno, M. Chanson, J. Anumonwo, I. Scerri, H. Gu, S.M. Taffet, M. Delmar, Role of the carboxyl terminal of connexin43 in transjunctional fast voltage gating, Circ. Res. 90 (4) (2002) 450–457.
[107] T.M. Suchyna, L.X. Xu, F. Gao, C.R. Fourtner, B.J. Nicholson, Identification of a proline residue as a transduction element involved in voltage gating of gap junctions, Nature 365 (1993) 847–849.
[108] A. Pfahnl, G. Dahl, Localization of a voltage gate in connexin46 gap junction hemichannels, Biophys. J. 75 (5) (1998) 2323–2331.
[109] V. Valiunas, D. Manthey, R. Vogel, K. Willecke, R. Weingart, Biophysical properties of mouse connexin30 gap junction channels studied in transfected human HeLa cells, J. Physiol. (Lond.) 519 (Pt 3) (1999) 631–644.
[110] C. Peracchia, X.G. Wang, L.L. Peracchia, Is the chemical gate of connexins voltage sensitive? Behavior of Cx32 wild-type and mutant channels, Am. J. Physiol. 276 (6 Pt 1) (1999) C1361–C1373.